

Институт за физику			
ПРИМЛЕНО: 22. 05. 2019			
Рад.јед.	бр.р.	Арх.шифра	Прилог
0801	73211		

Научном већу Института за физику Београд

Београд, 22. мај 2019.

Предмет:

Молба за покретање поступка за избор у звање истраживач сарадник

С обзиром да испуњавам критеријуме прописане од стране Министарства просвете, науке и технолошког развоја и Научног веће Института за физику у Београд за стицање звања истраживач сарадник, молим Научно веће Института за физику у Београду да покрене поступак за мој избор у наведено звање.

У прилогу достављам:

1. Мишљење руководиоца пројекта са предлогом чланова комисије за избор у звање
2. Стручну биографију
3. Преглед научне активности
4. Списак објављених научних радова и њихове копије
5. Потврду о уписаним докторским студијама
6. Копију диплома основних и мастер академских студија
7. Уверење о прихваћеној теми докторске дисертације

Са поштовањем,

Јадранка Васиљевић

Јадранка Васиљевић

Београд, 22. мај 2019. године

Предмет: Мишљење руководиоца пројекта о избору Јадранке Васиљевић у звање истраживач сарадник

Јадранка Васиљевић је ангажована на пројекту основних истраживања Министарства просвете, науке и технолошког развоја ОИ171036, под називом „*Нелинеарна фотоника нехомогених средина и површине*“. Од 2014. била је стипендиста Министарства просвете, науке и технолошког развоја. Запослена је у Лабораторији за нелинеарну фотонику у оквиру Националног центра за фотонику Института за физику у Београду од 2017 године.. На поменутом пројекту ради на темама простирања недифрагујућих Матјеових зрака као и простирању светlosti у Матјеовим фотонским решеткама у фоторефрактивној средини под руководством Др Драгане Јовић Савић. С обзиром да испуњава све предвиђене услове у складу са Правилником о поступку, начину вредновања и квантитативном исказивању научноистраживачких резултата Министарства просвете науке и технолошког развоја, сагласна сам са покретањем поступка и предлажем избор Јадранке Васиљевић у звање истраживач сарадник.

За састав комисије за избор Јадранке Васиљевић у звање истраживач сарадник предлажем:

- 1) др Драгана Јовић Савић, научни саветник, Институт за физику у Београду
- 2) др Дејан Тимотијевић, научни саветник, Институт за физику у Београду
- 3) проф др Ђорђе Спасојевић, редовни професор, Физички факултет Универзитета у Београду

Драгана Јовић Савић

Др Драгана Јовић Савић

Научни саветник

Руководилац пројекта ОИ171036

Биографија кандидата:

Јадранка Васиљевић рођена у Краљеву 27. маја 1990. године где је завршила основну и средњу школу. Основне академске студије уписала је 2009. а завршила их 2013. године на Природно-математичком факултету Универзитета у Крагујевцу, смер Физика са просечном оценом 9,51. Исте године уписала је мастер академске студије на Природно-математичком факултету Универзитета у Крагујевцу, смер Физика, које је завршила 2014. године са просечном оценом 9,5. Завршним рад под називом: „*Простирање и локализација светлости у квазипериодичним фотонским решеткама*”, чији експериментални део је одрадила је на Институту за физику у Лабораторији за нелинеарну фотонику под менторством Др Драгане Јовић Савић а одбранила га је 2014. године на Природно-математичком факултету Универзитета у Крагујевцу.

Школске 2014/2015. године Јадранка је уписала Докторске академске студије на Физичком факултету Универзитета у Београду, студијски програм Квантна оптика и ласери. Кандидат је започео истраживачки рад на Институту за физику Београд у Лабораторији за нелинеарну фотонику. Тема докторске дисертације под називом „*Простирање, локализација и контрола светлости у Матјеовим решеткама*“ јој је одобрена на састанку Колегијума докторских студија одржаном дана 08. 05. 2019. године.

Од априла 2015. до новембра 2017. године била је стипендиста Министарства просвете, науке и технолошког развоја. Од новембра 2017. године запослена је на Институту за физику у Београду на позицији истраживач приправник у Лабораторији за нелинеарну фотонику, где је ангажована на пројекту основних истраживања ОИ171036 „*Нелинеарна фотоника нехомогених средина и површина*“ Министарства просвете, науке и технолошког развоја Републике Србије чији руководијац је Др Драгана Јовић Савић. Поред тога учествовала је и на билатералном пројекту између Републике Србије и Републике Немачке „*Контрола светлости помоћу детерминистичких апериодичних и комплексних фотонских решетки*“ 2016. и 2017. године, у оквиру ког је више пута посетила Институт за примењену физику, Универзитета у Минстеру, Немачка.

Њена област истраживања је нелинеарна фотоника. Резултате свог истраживања публиковала је у пет радова. Један рад у међународном часопису изузетних вредности (категорија M21a) три рада у два врхунска међународна часописа (категорија M21) и један рад у истакнутом међународном часопису (категорија M22) као и 3 саопштења са међународних скупова штампана у изводу (M34).

Преглед научне активности

Научна активност Јадранке Васиљевић односи се на нелинеарну фотонику: испитивање феномена који се односе на процес интеракције ласерског зрачења са нелинеарном оптичком средином, истраживање ефеката приликом простирања светлости у сложеним фотонским решеткама, изучавање класе недифрагујућих Матјеових зрака у различитим нелинеарним срединама, као и експерименталну реализацију фотонских решетки помоћу ових зрака, како периодичних тако и квазипериодичних, уз помоћ оптички индуковане технике, и изучавање феномеана простирања и локализације светлости у њима, с акценотом на њихове потенцијалне примене.

Досадашњи научно истраживачки рад Јадранке Васиљевић, базиран на горе поменутим проблемима, може се класификовати у следеће основне правце:

1. Изучавање простирања и локализације светлосног таласа у једнодимензионалним квазипериодичним решеткама, формираним према правилима Фиbonачијеве речи.
2. Проучавање феномена при простирању Матјеових зрака у нелинеарној фоторефрактивној средини.
3. Вођење светлосног таласа у појединачним Матјеовим фотонским решеткама.
4. Формирање сложених фотонских решетки помоћу више Матјеових зрака.

1. Изучавање простирања и локализације светлосног таласа у једнодимензионалним квазипериодичним решеткама, формираним према правилима Фиbonачијеве речи

Током израде мастер рада кандидат је теоријски, нумерички и експериментално изучавао простирања и локализацију ласерске светлости у једнодимензионалним квазипериодичним решеткама, формираним према правилима Фиbonачијеве речи. Два Фиbonачијева елемента А и Б, коришћена су као растојања између таласовода. Оптички индукованом техником направљена је једнодимензионална Фиbonачијева решетка експериментално, у фоторефрактивном кристалу литијум ниобата, допираном гвожђем ($0,05\% \text{ Fe:LiNbO}_3$).

Демонстрирано је како нумерички тако и експериментално да је ширење таласа у оваквим таласоводима ефективно редуковано у поређењу са периодичним таласоводима. Разматран је и утицај промене индекса преламања на ширење таласа у оваквим системима. Доста израженија дифракција се јавља за мање промене индекса преламања.

2. Проучавање феномена при простирању Матјеових зрака у нелинеарној фоторефрактивној средини

У оквиру докторских студија Јадранка се бавила изучавањем недифрагујућих зрака пре свега класом од посебног интереса као што су Матјеови зраци. Акценат је стављен на примену ових зрака у нелинеарној оптици као и на услове за формирање различитих

фотонских решетки уз помоћ оваквих зрака како теоријски тако и експериментално. У експерименталној реализацији коришћена је техника оптичке индукције за уписивање фотонске решетке у фоторефрактивном кристалу стронцијум баријум ниобату допираним церијумом. Нумеричке симулације служиле су за егзактно симулирање експеримента али и проналажење интереснатах феномена који би се поновили у експерименту.

Експериментално и нумерички испитивано је нелинеарно простирање појединачних и елиптичних Матјеових зрака у фоторефрактивном кристалу. Испитивањем простирање појединачних Матјеових зрака нижег и вишег реда пронађени су ефекти слични дискретној дифракцији при преласку са једнодимензионалног на дводимензионални систем.

Након тога изучавани су елиптични Матјеови зраци у разним нелинеарним режимима како би се откриле стабилне или динамичке структуре. Нумерички су рачунате релевантне физичке величине, као што су орбитални ангуларни моменти и Поинтингов вектор као погодна величина за мерење тока енергије код динамичких структура. Утврђено је да се при простирању елиптичних Матјеових зрака у нелинеарној средини формирају хирални таласоводи. Променом параметара нелинеарности и величине Матјеовог зрака могуће је контролисати величину и закривљеност хиралних таласовода. Нумерички предвиђени резултати експериментално су потврђени.

3. Вођење светлосног таласа у појединачним Матјеовим фотонским решеткама

Кандидат се бавио и испитивањем простирање елиптичних оптичких вортекса кроз одређене врсте Матјеових решетки. Демонстриране су нове вортексне структуре као што су стабилне вортексне огрлице, код којих се облик и величина фрагмената огрлице могу контролисати променом реда или елиптичности Матјеове решетке. Повећањем нелинеарности формирају се осцилаторни диполи или динамичке нестабилности.

4. Формирање сложених фотонских решетки помоћу више Матјеових зрака

Јадранка је испитвала и услове за формирање фотонских решетки у фоторефрактивном кристалу стронцијум баријум ниобату коришћењем појединачних Матјеових зрака или интерференције више Матјеових зрака. Интерференцијом више Матјеових зрака различитог реда или интерференцијом више Матјеових зрака истог реда ротираних један у односу на други или на различитом растојању стварају се основни обрасци за формирање нових класа апериодичних решетки.

Списак радова кандидата Јадранке Васиљевић

РАДОВИ У МЕЂУНАРОДНИМ ЧАСОПИСИМА ИЗУЗЕТНИХ ВРЕДНОСТИ М21а

1. Alessandro Zannotti, **J. M. Vasiljević**, D. V. Timotijević, D. M. Jović Savić and Cornelia Denz, "Visualizing the Energy Flow of Tailored Light", Advanced Optical Materials 6(8), 1701355 (2018). DOI: 10.1002/adom.201701355
(M21a, IF= 7.430)

РАДОВИ У ВРХУНСКИМ МЕЂУНАРОДНИМ ЧАСОПИСИМА М21

1. Alessandro Zannotti, **J. M. Vasiljević**, D. V. Timotijević, D. M. Jović Savić, and Cornelia Denz, "Morphing discrete diffraction in nonlinear Mathieu lattices", Optics Letters, Vol. 44(7), 1592 - 1595, (2019). DOI: 10.1364/OL.44.001592
(M21, IF= 3.589)
2. **J. M. Vasiljević**, Alessandro Zannotti, D. V. Timotijević, Cornelia Denz and D. M. Jović Savić, "Elliptical vortex necklaces in Mathieu lattices", Phys. Rev. A 97, 033848 (2018). DOI: 10.1103/PhysRevA.97.033848
(M21, IF= 2.909)
3. **J. M. Vasiljević**, Alessandro Zannotti, D. V. Timotijević, Cornelia Denz and D. M. Jović Savić, "Creating aperiodic photonic structures by synthesized Mathieu-Gauss beams", Phys. Rev. A 96, 023840 (2017). DOI: 10.1103/PhysRevA.96.023840
(M21, IF= 2.909)

РАДОВИ У ИСТАКНУТИМ МЕЂУНАРОДНИМ ЧАСОПИСИМА М22

1. N. M. Lučić, D. M. Jović Savić, A. Piper, D. Ž. Grujić, **J. M. Vasiljević**, D. V. Pantelić, B. M. Jelenković, and D. V. Timotijević, "Light propagation in quasi-periodic Fibonacci waveguide arrays", Journal of the Optical Society of America B 32, 1510 (2015). DOI: 10.1364/JOSAB.32.001510
(M22, IF=1.731)

САОПШТЕЊА СА МЕЂУНАРОДНИХ СКУПОВА ШТАМПАНА У ИЗВОДУ М34

1. Marius Rimmer, Alessandro Zannotti, **J. M. Vasiljević**, D. V. Timotijevic, D. M. Jović Savić, Cornelia Denz, „Chirality and discrete diffraction in nonlinear Mathieu lattices“, SPIE Photonics Europe, Strasbourg, France, April 22-26, pp 75 (2018). **(M34)**
2. **J. M. Vasiljević**, Alessandro Zannotti, D. V. Timotijević, Cornelia Denz and D. M. Jović Savić, „Realizing aperiodic photonic lattices by synthesized Mathieu-Gauss beams“, VI International School and Conference of Photonics, Belgrade, Serbia, August 28-September 1 (2017). ISBN 978-86-82441-46-5 **(M34)**
3. **J. M. Vasiljević**, N. M. Lučić, D. V. Timotijević, A. Piper, D. Ž. Grujić, D. V. Pantelić, B. M. Jelenković and D. M. Jović Savić, „Light propagation in deterministic aperiodic Fibonacci waveguide arrays“, V International School and Conference on Photonics, Belgrade, Serbia, August 24-28 (2015). ISBN 978-86-7306-131-3 **(M34)**



Optics Letters

Morphing discrete diffraction in nonlinear Mathieu lattices

ALESSANDRO ZANNOTTI,^{1,*} JADRANKA M. VASILJEVIĆ,² DEJAN V. TIMOTIJEVIĆ,^{2,3}
DRAGANA M. JOVIĆ SAVIĆ,² AND CORNELIA DENZ¹

¹Institute of Applied Physics and Center for Nonlinear Science (CeNoS), University of Muenster, 48149 Muenster, Germany

²Institute of Physics, University of Belgrade, P.O. Box 68, 11001 Belgrade, Serbia

³Science Program, Texas A&M University at Qatar, P.O. Box 23874 Doha, Qatar

*Corresponding author: a.zannotti@uni-muenster.de

Received 14 January 2019; revised 20 February 2019; accepted 22 February 2019; posted 22 February 2019 (Doc. ID 357502); published 20 March 2019

Discrete optical gratings are essential components to customize structured light waves, determined by the band structure of the periodic potential. Beyond fabricating static devices, light-driven diffraction management requires nonlinear materials. Up to now, nonlinear self-action has been limited mainly to discrete spatial solitons. Discrete solitons, however, are restricted to the eigenstates of the photonic lattice. Here, we control light formation by nonlinear discrete diffraction, allowing for versatile output diffraction states. We observe morphing of diffraction structures for discrete Mathieu beams propagating nonlinearly in photosensitive media. The self-action of a zero-order Mathieu beam in a nonlinear medium shows characteristics similar to discrete diffraction in one-dimensional waveguide arrays. Mathieu beams of higher orders show discrete diffraction along curved paths, showing the fingerprint of respective two-dimensional photonic lattices. © 2019 Optical Society of America

<https://doi.org/10.1364/OL.44.001592>

Manipulating waves by customizing their interaction with functional materials enables a variety of photonic applications, e.g., tailored diffraction at gratings to discretize the waves' spectral components [1,2]. Waves in periodically structured media show dynamics that cannot be realized in homogeneous media, determined by the media's band structure. Propagation of light in dielectric media with a periodically varying refractive index can mimic the spatio-temporal characteristics that are typically encountered in discrete systems, and the underlying field evolution effectively becomes "discretized" [1]. Most importantly, the vision to control light with light is realizable only by exploiting nonlinear materials as mediators [3]. Thus, shaping the periodically varying refractive index structure allows for diffraction management to control in turn the light distribution [4].

Different types of periodic photonic structures, including arrays of evanescently coupled optical waveguides [5], optically induced lattices in photorefractive materials [6], and photonic crystals [7], have been employed to engineer and control

fundamental properties of wave propagation. Arrays or lattices of evanescently coupled waveguides are prime examples of structures in which *discrete diffraction* [2,5,8] can be observed. These arrays consist of equally spaced identical waveguide elements or sites, possessing all essential characteristics of a photonic crystal structure (Brillouin zones, band structure, etc.). In such a physical setting, light couples between waveguides through tunneling, showing its diffraction characteristics. When low intensity light is injected into one or a few neighboring waveguides, it couples to more and more waveguides, broadening its spatial distribution. Fundamentally new physics occur in contrast to diffraction in homogeneous media. High-intensity light producing nonlinear responses in the refractive index is capable of forming *discrete spatial solitons* [9]. A renewed interest in nonlinear light-matter interaction goes beyond soliton formation. It is devoted to physical systems with dimensionality morphing, e.g., the continuous transformation of the lattice structure from 1D to 2D [10–12].

Nondiffracting beams, having propagation-invariant intensity distributions, allow creating 1D and 2D photonic lattices in photosensitive media. Particularly in the areas of optics and atom physics, these beams enable novel applications [13–16]. Among the variety of different nondiffracting beams, Mathieu beams [15,17] solve the Helmholtz equation in elliptic cylindrical coordinates [18]. They are used for a new type of optical lattice-writing light [19–23] allowing solitons or even elliptically shaped vortex solitons, and are beneficially used for particle manipulation [24]. However, their elliptical characteristics allow going far beyond soliton investigations and extending applications of nonlinear self-action.

In this Letter, we exploit Mathieu beams as lattice-writing light to fabricate discrete waveguide structures and investigate their nonlinear self-action in these structures, leading to morphing discrete diffraction. We investigate Mathieu beams of different orders in a photorefractive crystal, experimentally and numerically. We link linear discrete diffraction with nonlinear self-effects and demonstrate gradual transition from one to two dimensions. We use the term *morphing diffraction* to describe the nonlinear behavior similar to discrete diffraction.

We observe discrete diffraction similar to the typical discrete diffraction observed in 1D waveguide arrays, with Mathieu beams of zeroth order propagating in nonlinear media. For lower nonlinearity, we observe a behavior similar to broad Gaussian beam diffraction in waveguide arrays. Increasing the order of Mathieu beams, we demonstrate dimensionality morphing of discrete diffraction, with a gradual transition from 1D to 2D waveguiding geometries. With higher-order Mathieu beams, we observe discrete diffraction along each layer. For higher nonlinearities, we observe reflection along one transverse direction and asymmetric intensity distributions due to the thermal diffusive effects.

To experimentally investigate the nonlinear propagation of Mathieu beams, we use the setup shown in Fig. 1. A frequency-doubled Nd:YVO₄ laser illuminates a spatial light modulator (SLM) "Holoeye Pluto" and is modulated in both amplitude and phase [25]. An appropriate Fourier filter (FF) is implemented. The extraordinary polarized structure beam interacts with the photorefractive strontium barium niobate (SBN) crystal, which has dimensions of $5 \times 5 \times 15$ mm³. It is externally biased with an electric field $E_{\text{ext}} = 1600$ V cm⁻¹ parallel to the optical c axis, directed along one of the shorter axes, parallel to the x axis. The propagation of the paraxial light fields is mainly in z direction. An adjustable microscope objective and a camera build the imaging system to scan the entire intensity volume by recording single transverse slices. In order to measure the phase of the structure beam, we superimpose a tilted plane wave as a reference beam and use a standard digital holographic method.

We simulate the light propagation in a nonlinear photorefractive medium by solving the nonlinear Schrödinger equation (1) numerically using a spectral split-step propagation method [26]:

$$i\partial_z\psi(\mathbf{r}) + \frac{1}{2k_z}[\Delta_{\perp} + V(I)]\psi(\mathbf{r}) = 0. \quad (1)$$

The nonlinear light–matter interaction is calculated by assuming a light-induced refractive index modulation as proposed in [27]. The paraxial scalar light field $\psi(\mathbf{r})$ with longitudinal wave vector k_z propagates in a nonlinear potential $V(I) = -k_z^2 n_e^2 r_{33} E_{sc}(I)$ defined by photorefractive nonlinearity. The laser wavelength $\lambda = 532$ nm defines the wave number $k = 2\pi/\lambda = \sqrt{k_t^2 + k_z^2}$. $n_e = 2.358$ is the extraordinary bulk refractive index and $r_{33} = 237$ pm V⁻¹ the corresponding linear electro-optic coefficient. The electric space charge field $E_{sc}(I)$ builds up inside the SBN crystal and depends on the intensity $I = |\psi(\mathbf{r})|^2$. We model the nonlinear optical induction of the intensity-dependent, saturable, non-local, and anisotropic refractive index modulation [28], as shown in our previous works [23,29].

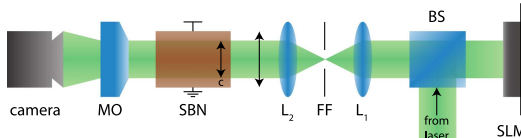


Fig. 1. Scheme of experimental setup. BS, beam splitter; FF, Fourier filter; L, lens; MO, microscope objective; SLM, phase-only spatial light modulator.

We use even Mathieu beams $\psi_m(\xi, \eta)$ [15], mathematically described as a product of radial c_{em} and angular J_{em} Mathieu functions of order m :

$$\psi_m(\xi, \eta) = C_m(q)J_{\text{em}}(\xi; q)c_{\text{em}}(\eta; q), \quad (2)$$

where $C_m(q)$ is a weighting constant that depends on $q = f^2 k_t^2 / 4$, a parameter of ellipticity which is related to the positions f of the two foci and the transverse wave number $k_t = 2\pi/a$, where a is a characteristic structure size. ξ and η are elliptical coordinates and their relation with spatial coordinates x, y is given by $x + iy = f \cosh(+i\eta)$. Here we choose $a = 25$ μm.

Before investigating the nonlinear propagation of Mathieu beams, we exemplarily characterize the free-space propagation of a zeroth-order even Mathieu writing beam with $q = 25$ experimentally. The quasi 1D discrete intensity distribution is shown in Fig. 2(A1), accompanied by the phase pattern (A2). It propagates invariantly (A3) over a distance of 6.36 mm in free space, which corresponds to 15 mm in the homogeneous SBN crystal. The same conclusions are worthy for higher-order Mathieu beams used later to demonstrate intermediate and 2D discrete diffraction.

Their discrete intensity distribution with a complex transverse curvature makes Mathieu beams highly suited to investigate morphing diffraction in self-induced waveguides. We find that the lattice-fabricating Mathieu beam in Fig. 2 shows *nonlinear discrete diffraction* as a consequence of its self-action in dependence of the beam power P that influences the strength of the nonlinearity, shown in Fig. 3. The first row depicts the

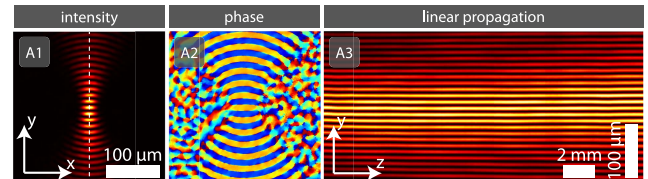


Fig. 2. Experimental characterization of a zeroth-order lattice fabricating even Mathieu beam. (A1) Transverse intensity and (A2) phase distributions. (A3) Cross section through the intensity volume at the orientation indicated with the white line in (A1).

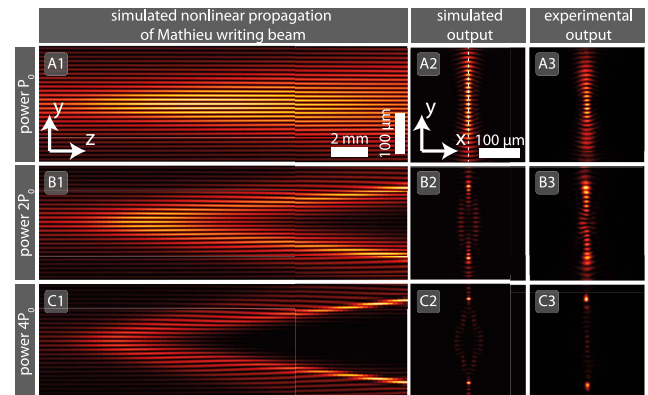


Fig. 3. (1) Simulated nonlinear propagation of Mathieu beams shows morphing discrete diffraction for increasing beam powers P . (2) Simulated and (3) experimentally observed intensity distributions at the crystal's back face.

simulated yz cross section through the intensity volume (A1), and further the simulated (A2) and the experimentally obtained (A3) transverse intensity distributions at the back face of the SBN crystal for $P = P_0 = 10 \mu\text{W}$, showing that the waveguides are well fabricated. The observed discrete diffraction has similarities to that of a broad Gaussian beam propagating in 1D periodic waveguide arrays [2]. By doubling the beam power twice [Figs. 3(B) and 3(C)], we observe a spreading of highest intensities away from the center and towards the outer parts along the y axis. This effect is the nonlinear counterpart of linear discrete diffraction in 1D waveguide arrays. Since the envelope of the 1D intensity distribution along the y axis of an initial zeroth-order Mathieu beam has its maximum in the origin, the refractive index modulation and thus the self-action of the writing beam is strongest in the center. Very high beam powers of $4P_0$ increase diffusive effects [23,29] along the optical c axis, parallel to the x axis, apparent at the shift in intensity in (B3) and (C3).

Beyond 1D nonlinear discrete diffraction, we realize morphing discrete diffraction along curved 2D paths at the example of Mathieu lattices showing dimensionality crossover. We chose

the sixth-order even Mathieu beam with $q = 325$ [10–12], imaged in Fig. 4, for demonstration of dimensionality crossover. The figure shows the simulated (A) and experimentally observed (B) transverse intensity distributions at the back face of the SBN crystal in dependence of a successive doubling of the initial beam power $P_0 = 10 \mu\text{W}$. We observe intensity distributions that reflect the fingerprint of linear discrete diffraction; however, the outward directed intensity transport in the nonlinear lattices follows mainly along each hyperbolic layer of the Mathieu beam (C).

For the lowest power P_0 , the highest intensities located in the center of an initial sixth-order Mathieu beam are redistributed towards the outer parts in y direction, shown by the intensity profile along the green line (B1) and (C1). Increasing the power P , we observe that further hyperbolic arms of the Mathieu lattice are affected. Central intensities spread outwards along 2D curves (2 and 3). Additionally, a diffusion driven shift in x direction and merging intensities due to modulation instabilities influence the intensity redistribution; however, the pure effect of 2D nonlinear discrete diffraction along hyperbolic paths is predominantly observable.

To demonstrate that discrete Mathieu lattices themselves imprint the intensity distribution on probing light that is typical for discrete diffraction, we simulate linear propagation of narrow Gaussian beams in the lattices presented above. Figure 5(A) images the intensity distribution of such a Gaussian probe beam inside the Mathieu lattice in Fig. 3(A). The initial plane in Fig. 5(A) indicates the lattice. The perpendicularly launched probe beam couples from waveguide to waveguide, presenting diffraction characteristics as in 1D waveguide arrays. Further configurations are launching probe beams in the 2D lattice in Fig. 4(A1) in the center and the outermost layer [purple hyperbola in Fig. 4(B1)]. The intensity of the central excitation diffracts discrete in central and neighboring layers, shown in (B). The outer excitation evolves to discrete diffraction along the hyperbolic waveguide layer, imaged in (C).

In summary, we demonstrated morphing diffraction of Mathieu beams with transition from 1D to 2D. These nondiffracting beams allow realizing discrete lattices in general elliptic geometries. We showed that discrete diffraction on unconventional paths is possible as a result of the self-action of Mathieu beams in nonlinear material. We observed discrete diffraction similar to that observed in 1D waveguide arrays using Mathieu beams of zeroth order, or discrete diffraction similar to the one in 2D photonic lattices with higher-order Mathieu beams. Increasing the nonlinearity, reflections along one transverse direction are observed as well as asymmetric intensity distributions due to thermal diffusive effects. Thus, nonlinear discrete

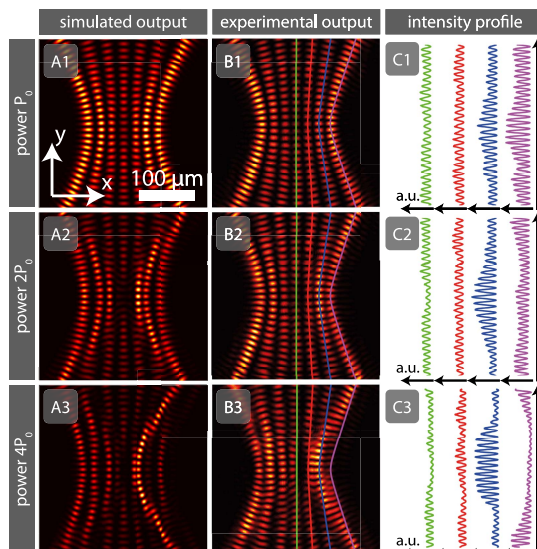


Fig. 4. Morphing discrete diffraction on curved paths based on the self-action of sixth-order even Mathieu beams: (A) simulated and (B) experimentally observed transverse intensity distributions at the crystal's back face. (C) Intensity profiles along the hyperbolic waveguide layers indicated in (B).

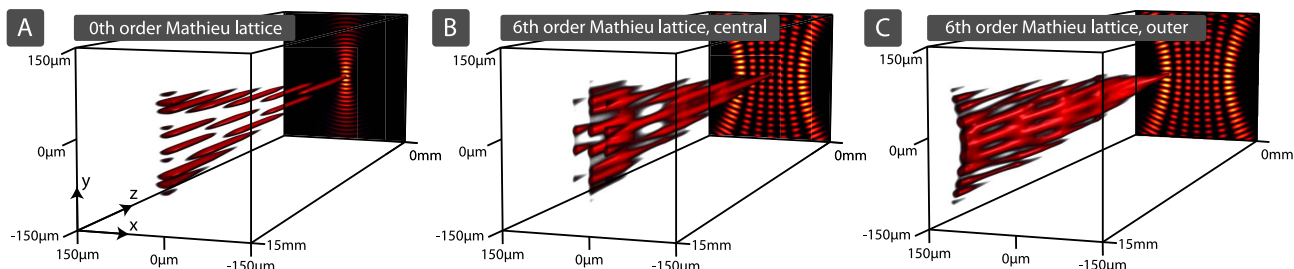


Fig. 5. Gaussian probe beam in Mathieu lattice potentials from: (A) Fig. 3(A1); (B) Fig. 4(B1) central waveguides; (C) Fig. 4(B1) purple waveguide layer.

diffraction allows controlling the light dynamics in lattices by light itself, providing a simple technique to create novel gratings and nonlinear switches.

Funding. Deutscher Akademischer Austauschdienst (DAAD) (57219089); Ministarstvo Prosvete, Nauke i Tehnološkog Razvoja (OI 171036); Qatar National Research Fund (QNRF) (NPRP 8-028-1-001).

REFERENCES

1. H. S. Eisenberg, Y. Silberberg, R. Morandotti, and J. S. Aitchison, *Phys. Rev. Lett.* **85**, 1863 (2000).
2. T. Pertsch, T. Zentgraf, U. Peschel, A. Brauer, and F. Lederer, *Phys. Rev. Lett.* **88**, 093901 (2002).
3. J. Hudock, N. K. Efremidis, and D. N. Christodoulides, *Opt. Lett.* **29**, 268 (2004).
4. D. N. Christodoulides, F. Lederer, and Y. Silberberg, *Nature* **424**, 817 (2003).
5. H. S. Eisenberg, Y. Silberberg, R. Morandotti, A. R. Boyd, and J. S. Aitchison, *Phys. Rev. Lett.* **81**, 3383 (1998).
6. J. W. Fleischer, M. Segev, N. K. Efremidis, and D. N. Christodoulides, *Nature* **422**, 147 (2003).
7. J. D. Joannopoulos, S. G. Johnson, J. N. Winn, and R. D. Meade, *Fotonic Crystals: Molding the Flow of Light*, 2nd ed. (Princeton University, 1995).
8. T. Pertsch, U. Peschel, F. Lederer, J. Burghoff, M. Will, S. Nolte, and A. Tünnermann, *Opt. Lett.* **29**, 468 (2004).
9. F. Lederer, G. I. Stegeman, D. N. Christodoulides, G. Assanto, M. Segev, and Y. Silberberg, *Phys. Rep.* **463**, 1 (2008).
10. A. Szameit, Y. V. Kartashov, F. Dreisow, M. Heinrich, T. Petrich, S. Nolte, A. Tünnermann, V. A. Vysloukh, F. Lederer, and L. Torner, *Phys. Rev. Lett.* **102**, 063902 (2009).
11. D. M. Jović, M. R. Belić, and C. Denz, *Phys. Rev. A* **84**, 043811 (2011).
12. U. Naether, Y. V. Kartashov, V. A. Vysloukh, S. Nolte, A. Tünnermann, L. Torner, and A. Szameit, *Opt. Lett.* **37**, 593 (2012).
13. J. Durnin, J. J. Miceli, and J. H. Eberly, *J. Opt. Soc. Am. A* **4**, 651 (1987).
14. J. Durnin, J. J. Miceli, and J. H. Eberly, *Phys. Rev. Lett.* **58**, 1499 (1987).
15. J. C. Gutiérrez-Vega, M. D. Iturbe-Castillo, and S. Chávez-Cerda, *Opt. Lett.* **25**, 1493 (2000).
16. M. A. Bandres, J. C. Gutiérrez-Vega, and S. Chávez-Cerda, *Opt. Lett.* **29**, 44 (2004).
17. J. C. Gutiérrez-Vega, M. D. Iturbe-Castillo, G. A. Ramírez, E. Tepichín, R. M. Rodríguez-Dagnino, S. Chávez-Cerda, and G. H. C. New, *Opt. Commun.* **195**, 35 (2001).
18. J. C. Gutiérrez-Vega, M. A. Meneses-Neva, and S. Chávez-Cerda, *Am. J. Phys.* **71**, 233 (2003).
19. P. Rose, M. Boguslawski, and C. Denz, *New J. Phys.* **14**, 033018 (2012).
20. Y. I. Kartashov, A. A. Egorov, V. A. Vysloukh, and L. Torner, *Opt. Lett.* **31**, 238 (2006).
21. F. Ye, D. Mihalache, and B. Hu, *Phys. Rev. A* **79**, 053852 (2009).
22. A. Ruelas, S. Lopez-Aguayo, and J. C. Gutiérrez-Vega, *Opt. Lett.* **33**, 2785 (2008).
23. J. V. Vasiljević, A. Zannotti, D. V. Timotijević, C. Denz, and D. M. Jović, *Phys. Rev. A* **96**, 023840 (2017).
24. C. Alpmann, R. Bowman, M. Woerdemann, M. Padgett, and C. Denz, *Opt. Express* **18**, 26084 (2010).
25. J. A. Davis, D. M. Cottrell, J. Campos, M. J. Yzuel, and I. Moreno, *Appl. Opt.* **38**, 5004 (1999).
26. G. Agrawal, *Nonlinear Fiber Optics*, 5th ed. (Academic, 2012).
27. N. V. Kukhtarev, V. B. Markov, S. G. Odulov, M. S. Soskin, and V. L. Vinetskii, *Ferroelectrics* **22**, 949 (1979).
28. A. A. Zozulya and D. Z. Anderson, *Phys. Rev. A* **51**, 1520 (1995).
29. A. Zannotti, J. V. Vasiljević, D. V. Timotijević, C. Denz, and D. M. Jović, *Adv. Opt. Mater.* **6**, 1701355 (2018).

Visualizing the Energy Flow of Tailored Light

Alessandro Zannotti,* Jadranka M. Vasiljević, Dejan V. Timotijević, Dragana M. Jović Savić, and Cornelia Denz

Exploiting the energy flow of light fields is an essential key to tailor complex optical multistate spin and orbital angular momentum (OAM) dynamics. With this work, the energy flow is identified and quantified by a novel approach that is based on the symmetry breaking induced by nonlinear light–matter interaction of OAM carrying beams at the example of Mathieu beams, showing transverse invariant intensity distributions. These complex scalar nondiffracting beams exhibit outstanding transverse energy flows on elliptic paths. Although their energy is continuously redistributed during linear propagation in homogeneous media, the beams stay nondiffracting. This approach to visualize the energy flow of light is based on the nonlinear self-action in a nonlinear crystal. By this, the sensitive equilibrium is perturbed and accumulation of rotating high-intensity spots is enabled. Intensity distributions on elliptic, chiral paths are demonstrated as a manifestation of the energy flow. Furthermore, the formation of corresponding refractive index modulations that may be implemented as chiral waveguides, is controlled via the beam power and structure size.

1. Introduction

The energy flow of light is determined by both, its spin angular momentum and its orbital angular momentum (OAM), and is generally described by the Poynting vector.^[1] Controlling the spatial polarization and phase structure of light, the combination of binary spin states and multistate orbital angular momentum dynamics is an essential key to further establish modern high-dimensional singular optics. These abilities enabled breakthrough research in the areas of spatial polarization modulation,^[2] classical entanglement,^[3] high-density signal transmission,^[4] or optical micromanipulation.^[5,6]

In order to investigate two-dimensional energy flows in the transverse plane, in particular nondiffracting beams with

A. Zannotti, Prof. C. Denz
Institute of Applied Physics and Center for Nonlinear Science (CeNoS)
Westfälische Wilhelms-Universität Münster
48149 Münster, Germany
E-mail: a.zannotti@uni-muenster.de

J. M. Vasiljević, Prof. D. V. Timotijević, Prof. D. M. Jović Savić
Institute of Physics
University of Belgrade
P.O. Box 68, 11001 Belgrade, Serbia
Prof. D. V. Timotijević
Science Program
Texas A&M University at Qatar
P.O. Box 23874, Doha, Qatar

DOI: 10.1002/adom.201701355

transverse invariant intensity distributions and continuously modulated phase distributions are suited. The class of nondiffracting beams has attracted considerable interest and features not only applications in optics, but also in solid state and atom physics.^[7–11] A detailed understanding of their energy flows therefore is of high importance in many communities. However, the energy flow of continuously modulated nondiffracting beams withstands a direct observation because it is hidden for the case of linear propagation in homogeneous media. The transverse intensity distribution stays invariant and the energy flow is continuously redistributed.

Four nondiffracting beam families exist as solutions of the paraxial as well as the nonparaxial Helmholtz equation in different coordinate systems:^[12–17] Discrete beams in Cartesian, Bessel beams^[8] in spherical, Mathieu beams in elliptic, and

Weber beams in parabolic coordinates. Among these diverse families, Mathieu beams^[9,10,18,19] may be interpreted as a generalized beam class, capable to interpolate between Cartesian and spherical coordinates. In contrast to parabolic Weber beams, their transverse spatial intensity distributions can form closed paths on ellipses, with spatially structured orbital angular momenta^[6,20] showing periodic boundaries.

Mathieu beams are highly appealing to access fundamental physical effects in elliptical coordinates.^[21] In several studies, they have been beneficially used for particle manipulation,^[5] and served as lattice-writing light,^[22–26] featuring the nonlinear propagation of (vortex) solitons in these previously linearly induced elliptic lattices. However, the self-action of Mathieu beams in nonlinear media was not investigated until now.

Scalar even and odd Mathieu beams exhibit only real-valued field distributions. Their transverse Poynting vector therefore vanishes. In contrast, the complex superposition of even and odd Mathieu beams leads to generalized elliptic Mathieu beams, showing outstanding continuously modulated spatial phase distributions, i.e., OAM.^[5,6,20] Thus, for these beams a transverse energy flow is present. Until today, only a few works have addressed the energy flow in these complex spatially modulated beams with its unique OAM characteristics, e.g., using the OAM structure of Mathieu beams to transfer orbital angular momentum to particles that start to rotate.^[5,6,20]

With this work, we present an approach to visualize the energy flow of light at the example of elliptic Mathieu beams. We demonstrate experimentally and numerically that the

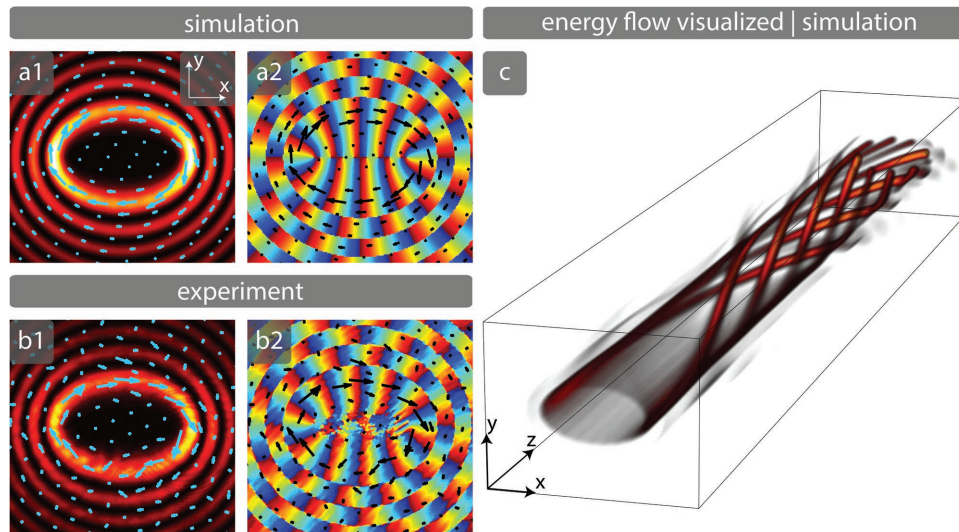


Figure 1. a,b) Poynting vector of the elliptic Mathieu beam and c) its nonlinear propagation. The energy flow, characterized by the Poynting vector (indicated by arrows), is (a) calculated and (b) observed experimentally for the initial beam profiles, shown in (a1, b1) intensity and (a2, b2) phase. The formation of rotating high-intensity filaments due to the nonlinear self-interaction is illustrated in (c).

energy flow of elliptic Mathieu beams becomes observable by propagating in a nonlinear photorefractive crystal. The nonlinearity breaks the sensitive equilibrium of the energy redistribution of the beam and enables the formation of high-intensity spots that encircle a common center, driven by the OAM in the direction of the energy flow. Due to the nonlinear interaction, the intensity distribution is transferred to a correspondingly twisted refractive index modulation. We demonstrate that we can control the formation and rotation of high-intensity spots by increasing the strength of the nonlinearity or by tailoring the size of the initial beam. Note, that by this, photonic structures can be implemented as chiral waveguides, supporting the actual and rich field of research on chiral photonic structures.^[27–31]

2. Characteristics of Elliptic Mathieu Beams

Fundamental Mathieu beams are solutions of the Helmholtz equation in elliptical cylindrical coordinates (ξ, η, z). They are mathematically described by a product of radial and angular Mathieu functions and exist either as even or odd solutions.^[9] Elliptic Mathieu beams represent a complex linear superposition of even and odd Mathieu beams of the same order m . For a monochromatic, scalar elliptic Mathieu beam of order m , the light field is given by^[21]

$$\psi(\xi, \eta) = C_m(q) J_{e_m}(\xi; q) c e_m(\eta; q) + i S_m(q) J_{o_m}(\xi; q) s e_m(\eta; q) \quad (1)$$

where J_{e_m} and J_{o_m} are the even and odd radial Mathieu functions, and $c e_m$ and $s e_m$ are the even and odd angular Mathieu functions of order m , respectively. $C_m(q)$ and $S_m(q)$ are weighting constants that depend on $q = f^2 k_t^2 / 4$ that in turn determines the ellipticity of the Mathieu beams. It is related to the positions f of the two foci and the transverse wave number $k_t = 2\pi/a$ that corresponds to a characteristic structure size a .

The transverse time-averaged Poynting vector $\langle \mathbf{S} \rangle$ of a linearly polarized, transverse light field ψ is determined by the spatial OAM distribution and given by^[32]

$$\langle \mathbf{S} \rangle = \frac{i\omega\epsilon_0}{2} (\psi^* \nabla \psi - \psi \nabla \psi^*) \quad (2)$$

where $\omega = ck$ is the angular-frequency that connects the speed of light c with the wave number $k = 2\pi/\lambda$, defined by the wavelength λ . ϵ_0 is the vacuum permittivity.

Figure 1 exemplarily shows an elliptic Mathieu beam of order $m = 10$ with an ellipticity of $q = 25$ (Panels (a,b)), and our concept to visualize its energy flow (Panel (c)). The numerically calculated transverse field as well as the experimentally obtained field are shown in intensity and phase at the initial plane in Figure 1a,b, respectively. While it is natural to calculate numerically an electric field ψ , experimentally only the transverse intensity (I) and phase (ϕ) are accessible. From these, we construct the experimentally obtained electric field $\psi = \sqrt{I} \exp[i\phi]$. Using Equation (2), we calculate and image the transverse Poynting vector of this beam, indicated with overlying arrows. Figure 1c shows a characteristic numerical simulation that illustrates how the main intensity that is distributed on an ellipse enters the front of a nonlinear crystal, optically induces a photonic structure that yields to the formation of high-intensity spots which start to rotate in the direction of the energy flow. At the back face of the crystal several spots remain that prove the existence of the initial energy flow.

In the following, we present our approach to visualize numerically and experimentally the energy flow of elliptic Mathieu beams and thus tailor the realization of chiral waveguides. We further demonstrate that we can control the rotation and the degree of filamentation mainly by the strength of the nonlinearity and the structure sizes of the Mathieu beams. In this work, we exemplary demonstrate our results for an elliptic Mathieu beam of order $m = 10$ and ellipticity $q = 25$. However,

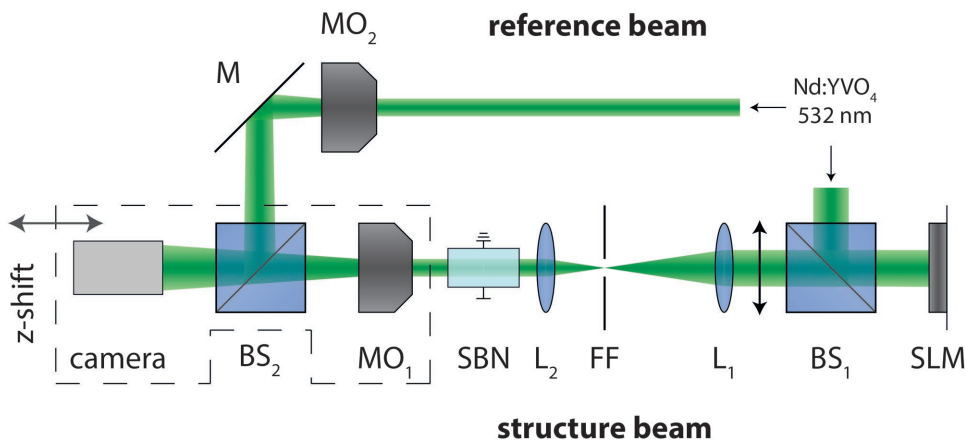


Figure 2. The experimental setup. BS: beam splitter, FF: Fourier filter, L: lens, M: mirror, MO: microscope objective, SLM: spatial light modulator.

realizations with elliptic Mathieu beams that differ in their order or ellipticity are possible within a certain parameter range that also depends on the further properties of the beam and the nonlinearity.

3. Details on the Numerical Simulations and the Experimental Setup

In the experiment, which is shown in Figure 2, we use a frequency-doubled Nd:YVO₄ laser. The broad laser beam illuminates as a plane wave a spatial light modulator “Holoeye Pluto VIS.” We adopt the method of Ref. [33] to modulate both, amplitude and phase of the initial transverse (*x*-*y*-plane) light field with one phase-only modulator. An appropriate Fourier filtering is required. The extraordinary polarized structure beams interact with a nonlinear Strontium Barium Niobate (SBN) crystal which has geometrical dimensions of 5 × 5 × 15 mm³. It is biased with an external electric field E_{ext} along the optical *c*-axis, directed along one of the shorter axis, parallel to the *x*-axis. The paraxial structured light field propagates mainly in *z*-direction. The intensity distribution at the back face of the SBN crystal is magnified with a microscope objective and imaged by a camera. In order to measure the phase of the structure beam, we superimpose a tilted plane wave as reference beam and use a digital holographic method.^[34]

Numerically, we solve the nonlinear Schrödinger Equation (3) by applying a spectral split step propagation method^[35,36]

$$i\partial_z\psi(\mathbf{r}) + \frac{1}{2k_z}[\Delta_\perp + V(I)]\psi(\mathbf{r}) = 0 \quad (3)$$

It describes the paraxial propagation of a scalar light field $\psi(\mathbf{r})$ with longitudinal wave vector k_z in a potential $V(I) = -k_z^2 n_e^2 r_{33} E(I)$ due to the photorefractive nonlinearity. $k = 2\pi/\lambda = (k_x^2 + k_y^2)^{1/2}$ is the wave number and defined by the wavelength $\lambda = 532$ nm. $n_e = 2.358$ is the extraordinary bulk refractive index, and $r_{33} = 237$ pm V⁻¹ is the corresponding electro-optic coefficient.

Photorefractive SBN provides a strong nonlinearity at comparatively low power levels and the ability of reversible

inductions. The electric field $E(I) = E_{\text{ext}} + E_{\text{sc}}(I)$ that builds up inside the SBN crystal is a superposition of a static external electric field $E_{\text{ext}} = 1600$ V cm⁻¹ and an internal space charge field $E_{\text{sc}}(I)$ that results due to the incident intensity distribution $I(r) = |\psi(r)|^2$.^[37] We calculate the resulting intensity-dependent, saturable, nonlocal, and anisotropic refractive index modulation via $E_{\text{sc}} = \partial_x \phi_{\text{sc}}$ by solving the modeling potential Equation (4) numerically.^[38]

$$\Delta\phi_{\text{sc}} + \nabla\phi_{\text{sc}} \nabla \ln(1+I) = E_{\text{ext}} \partial_x \ln(1+I) \quad (4)$$

4. Visualizing the Energy Flow of Elliptic Mathieu Beams

The balanced intensity redistribution of elliptic Mathieu beams is only present for their linear propagation in homogeneous media. We break this sensitive equilibrium by controlling the nonlinear self-action of elliptic Mathieu beams in a photorefractive crystal. When interacting with the optically induced refractive index modulation, the energy flow is altered. This leads to the accumulation of intensity at defined spots, where in turn the refractive index is increased. In this way, helically twisted refractive index lattices form and rotate in a predetermined direction.

Observing experimentally the formation and accumulation of high-intensity spots at the back face of the SBN crystal that are substantiated by corresponding numerical simulations and additionally controllable by the power and structure size of the writing beam represents our concept to visualize the energy flow of Mathieu beams. Furthermore, this method features the fabrication of chiral waveguide arrays.

We investigate the nonlinear self-action of the Mathieu beams with a structure size of $a = 15$ μm in the SBN crystal and reveal their energy flow by optically inducing a refractive index modulation with the structure beams. Based on the comparison with the numerical simulations, we estimate that the optically induced refractive index depth is in the order of 10⁻⁴. Systematically, we increase the initial beam power $P_0 \approx 20$ μW and double it in two steps in both, numerical simulation and

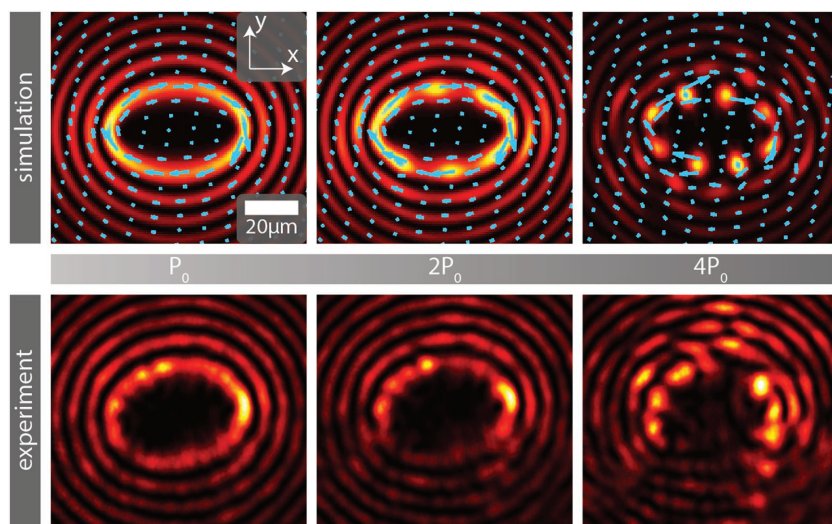


Figure 3. The transverse intensity distributions of elliptic Mathieu beams ($a = 15 \mu\text{m}$) at the back face of the SBN crystal, nonlinearly inscribed with increasing beam powers. Compared are numerical simulations (calculated Poynting vector indicated by arrows) with experimental results.

experiment. **Figure 3** shows the transverse intensity distributions at the back face of the SBN crystal. For the numerical simulations, we indicated with arrows that the Poynting vector (the energy flow) is still directed along the initial ellipse. Our construction scheme to experimentally obtain the complex electric field ψ and thus calculate the Poynting vector is not applicable here, since the spatial phase distribution ϕ is not accessible by using holographic techniques when imaging through the inhomogeneous refractive index modulation. As well, an experimental glance inside the crystal to see the 3D intensity distribution is not possible, since the light in the observing plane would be refracted by the inhomogeneous photonic structure in an unpredictable manner. Thus, we show that the experimental intensity distribution obtained at the back face of the crystal is tunable by changing the beam power so that spots of high intensity can be realized with changing positions and connect their individual manifestation with the formation of chiral lattices inside the crystal. The back face intensity distributions of simulation and experiment are in high agreement and substantiate our numerical simulations for the 3D distribution of the intensity inside the volume.

In particular, we show the transition from quasi linear propagation to a strong nonlinear self-interaction which introduces a symmetry breaking of the energy flow. For a weak beam power P_0 the beam propagates almost linearly, apparent at an almost unchanged output intensity distribution, indicating that the beam is still nondiffracting. When doubling the power, modulations emerge in form of occurring accumulations of intensity along the beforehand smoothly modulated ellipse. The writing beam thus can no longer be considered as nondiffracting nor as Mathieu beam. For the highest beam power of $4P_0$, separated spots of high intensity appear and rotate in the direction indicated by the Poynting vector, thereby forming rotating refractive index strands in analogy to the simulation in Figure 1c. The spots that occur at the back face of the SBN crystal are a consequence of modulation instabilities^[39] on an ellipse. Thus,

the amount of spots does not only depend on the order m of the elliptic Mathieu beams, but is influenced by several parameters, like the strength of the nonlinearity, the structure size, or the propagation distance.

Due to the modulation of the intensity distribution along the innermost ellipse and the anisotropic medium, the refractive index modulation is predominantly established in the direction of the optical c -axis. Subsequently, the energy flow, which is typically located on an ellipse, is now preferentially directed perpendicular to the c -axis where the refractive index modulation is weak, but is especially hindered to flow parallel to the c -axis due to the strong variations in the potential. Thus, conglomerations of high intensity form in particular at the trough of high refractive index where enough intensity is accumulated to create solitary strands of increased refractive index.

Note that these twisted photonic structures may act as waveguides for further probe beams and guide light on elliptical, chiral paths. Our numerical simulations and the experimental results both indicate that the period of rotation changes during formation as well as the radius from the central axis. Moreover, some streams of intensity branch and multiple intensity maxima occur (cf. Section 5). Our approach therefore provides a flexible and easy to implement method to realize chiral photonic media. Further investigations could potentially show advanced light-matter interactions, e.g., when probing these diverse chiral structures with chiral light.

5. Tailored, Nonlinear Mathieu Lattices

Additional to the previously discussed dependence of the formation of rotating waveguides on the strength of the nonlinearity, we demonstrate the control of the induction of elliptic Mathieu lattices in the nonlinear medium by changing the characteristic structure size $a = 2\pi/k_t$. Different elliptic Mathieu beams show a very rich rotating behavior with different spot characteristics.

Figure 4 shows the nonlinear control of the beam rotation by changing the beam size parameter a , whereby the beam power is constant at $P_0 \approx 20 \mu\text{W}$. We apply characteristic beam sizes of $a = [15, 20, 25] \mu\text{m}$. Compared are our experimental results with corresponding numerical simulations. Arrows again indicate the Poynting vector. We found that by increasing the structure size a of elliptic Mathieu beams, the local slope of the helix of the emerging rotating strands of higher refractive index is decreased. We also observe a coupling of the rotation to the quantity of spots. For $a = 15 \mu\text{m}$ in Figure 4, we hardly see conglomerations of intensity. For $a = 20 \mu\text{m}$ similar rotating waveguides occur as we have observed them for the structure size of $a = 15 \mu\text{m}$ with a power P that is comparable to be between $2P_0$ and $4P_0$, shown in Figure 3. By this, we find a regime where the strength of the nonlinearity is suited to

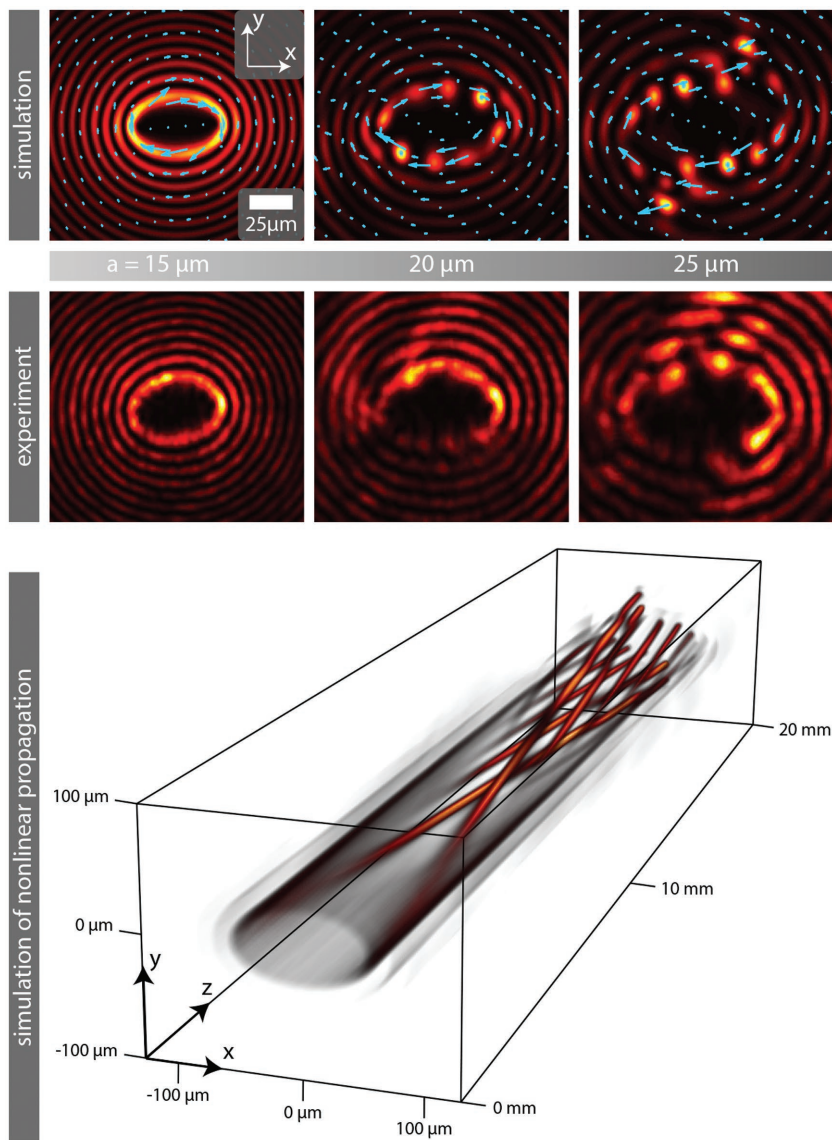


Figure 4. Numerically calculated (top) and experimentally measured (middle) transverse intensity distributions at the back face of the SBN crystal after nonlinear and self-interacting propagation of elliptic Mathieu beams ($P \approx 20 \mu\text{W}$), for beams with different structure sizes a . Arrows indicate the Poynting vector. The 3D intensity volume (bottom) visualizes the branching due to modulation instabilities on an ellipse for the case that $a = 25 \mu\text{m}$.

host the rotating photonic structures. This in turn is justified by the fact that for $a = 25 \mu\text{m}$ the self-action is strong and tends to become stronger for larger structure sizes a , also recognizable by the Poynting vector that directs outward for the outer high-intensity spots. Figure 4 shows the numerically simulated 3D intensity volume for $a = 25 \mu\text{m}$, and demonstrates exemplary for this borderline case the enhanced degree of branching for increased beam sizes. In the presented case, new branches of high intensity start to form after a propagation distance of about 10 mm and rotate. Further branches appear after longer propagation distances. Note that for larger structure sizes, the intensity spreads to ellipses located more outside due to increasing modulation instabilities of the broader beam. Thus,

rotating strands of high intensity can only induce chiral refractive index strands for these proper parameters.

6. Conclusion

We presented an approach to identify and visualize the energy flow of light based on the symmetry breaking by nonlinear light-matter interaction of OAM carrying beams. As an example, we chose elliptic Mathieu beams with outstanding continuously modulated OAM distributions. We used a nonlinearity introduced in form of a photorefractive SBN crystal in order to break the sensitive equilibrium, which is present for linear propagation of nondiffracting beams. We demonstrated exemplarily that the nonlinear self-action of elliptic Mathieu beams leads to the formation of high-intensity filaments, which rotated in the direction determined by the energy flow. The dependence of these emerging photonic structures on the strength of the nonlinearity and the structure size of the Mathieu beams was investigated and we pointed out that the twisted refractive index formation could act as chiral waveguides. We worked out that the formation of chiral Mathieu lattices is possible only in this limited regime with proper parameters for the nonlinearity and structure size. Corresponding numerical simulations substantiate our results. For elliptic Mathieu beams, our approach furthermore is well suited to fabricate rotating photonic structures with elliptic trajectories, thereby considerably advancing the field of chiral light and photonic structures.

Note that chiral lattices created by our approach show longitudinally increasing “helix slopes”, and additionally tailored transverse ellipticities. Both properties may be considered as novel degree of freedom to design unique band structures and realize artificial photonic media with new topologies.

Acknowledgements

The authors acknowledge support by the German Academic Exchange Service (Project 57219089), the Ministry of Education, Science, and Technological development, Republic of Serbia (Projects OI 171036), as well as the Qatar National Research Fund (NPRP 7-665-1-125).

Conflict of Interest

The authors declare no conflict of interest.

Keywords

chiral media, energy flow, Mathieu beams, nonlinear optics, photorefractive optics

Received: December 13, 2017

Revised: January 26, 2018

Published online:

- [1] M. Born, E. Wolf, *Principles of Optics*, 7th ed., Cambridge University Press, Cambridge, UK **1999**.
- [2] E. Otte, C. Alpmann, C. Denz, *J. Opt.* **2016**, *18*, 074012.
- [3] F. Töppel, A. Aiello, C. Marquardt, E. Giacobino, G. Leuchs, *New J. Phys.* **2014**, *16*, 073019.
- [4] J. Leach, M. J. Padgett, S. M. Barnett, S. Franke-Arnold, J. Courtial, *Phys. Rev. Lett.* **2002**, *88*, 257901.
- [5] C. Alpmann, R. Bowman, M. Woerdemann, M. Padgett, C. Denz, *Opt. Express* **2010**, *18*, 26084.
- [6] C. López-Mariscal, J. C. Gutiérrez-Vega, G. Milne, K. Dholakia, *Opt. Express* **2006**, *14*, 4182.
- [7] J. Durnin, *J. Opt. Soc. Am. A* **1987**, *4*, 651.
- [8] J. Durnin, J. J. Miceli, J. H. Eberly, *Phys. Rev. Lett.* **1987**, *58*, 1499.
- [9] J. C. Gutiérrez-Vega, M. D. Iturbe-Castillo, S. Chávez-Cerda, *Opt. Lett.* **2000**, *25*, 1493.
- [10] M. A. Bandres, J. C. Gutiérrez-Vega, S. Chávez-Cerda, *Opt. Lett.* **2004**, *29*, 44.
- [11] R. Stützle, M. C. Göbel, T. Hörner, E. Kierig, I. Mourachko, M. K. Oberthaler, M. A. Efremov, M. V. Fedorov, V. P. Yakovlev, K. A. H. van Leeuwen, W. P. Schleich, *Phys. Rev. Lett.* **2005**, *95*, 110405.
- [12] Z. Bouchal, *Czech J. Phys.* **2003**, *53*, 537.
- [13] P. Rose, M. Boguslawski, C. Denz, *New J. Phys.* **2012**, *14*, 033018.
- [14] U. Levy, S. Derevyanko, Y. Silberberg, *Prog. Opt.* **2016**, *61*, 237.
- [15] P. Zhang, Y. Hu, T. Li, D. Cannan, X. Yin, R. Morandotti, Z. Chen, X. Zhang, *Phys. Rev. Lett.* **2012**, *109*, 193901.
- [16] P. Aleahmad, M.-A. Miri, M. S. Mills, I. Kaminer, M. Segev, D. N. Christodoulides, *Phys. Rev. Lett.* **2012**, *109*, 203902.
- [17] M. Bandres, M. A. Alonso, I. Kaminer, M. Segev, *Opt. Express* **2013**, *21*, 13917.
- [18] J. C. Gutiérrez-Vega, M. D. Iturbe-Castillo, G. A. Ramírez, E. Tepichín, R. M. Rodríguez-Dagnino, S. Chávez-Cerda, G. H. C. New, *Opt. Commun.* **2001**, *195*, 35.
- [19] C. L. López-Mariscal, M. A. Bandres, J. C. Gutiérrez-Vega, S. Chávez-Cerda, *Opt. Express* **2005**, *13*, 2364.
- [20] S. Chávez-Cerda, M. J. Padgett, I. Allison, G. H. C. New, J. C. Gutiérrez-Vega, A. T. O'Neil, I. MacVicar, J. Courtial, *J. Opt. B: Quantum Semiclassical Opt.* **2001**, *195*, 35.
- [21] J. C. Gutiérrez-Vega, R. M. Rodríguez-Dagnino, M. a. Meneses-Nava, S. Chávez-Cerda, *Am. J. Phys.* **2003**, *71*, 233.
- [22] Y. V. Kartashov, V. A. Vysloukh, L. Torner, *Phys. Rev. Lett.* **2004**, *93*, 093904.
- [23] R. Fischer, D. N. Neshev, S. Lopez-Aguayo, A. S. Desyatnikov, A. A. Sukhorukov, W. Krolikowski, Y. S. Kivshar, *Opt. Express* **2006**, *14*, 2825.
- [24] Y. V. Kartashov, A. A. Egorov, V. A. Vysloukh, L. Torner, *Opt. Lett.* **2006**, *31*, 238.
- [25] F. Ye, D. Mihalache, B. Hu, *Phys. Rev. A* **2009**, *79*, 053852.
- [26] A. Ruelas, S. Lopez-Aguayo, J. C. Gutiérrez-Vega, *Opt. Lett.* **2008**, *33*, 2785.
- [27] A. Zannotti, F. Diebel, M. Boguslawski, C. Denz, *Adv. Opt. Mater.* **2016**, *5*, 1600629.
- [28] J. Becker, P. Rose, M. Boguslawski, C. Denz, *Opt. Express* **2011**, *19*, 9848.
- [29] J. Xavier, S. Vyas, P. Senthilkumaran, C. Denz, J. Joseph, *Opt. Lett.* **2011**, *36*, 3512.
- [30] A. Kuzyk, R. Schreiber, H. Zhang, A. Govorov, T. Liedl, N. Liu, *Nat. Mater.* **2014**, *13*, 862.
- [31] M. C. Rechtsman, J. M. Zeuner, Y. Plotnik, Y. Lumer, D. Podolsky, F. Dreisow, S. Nolte, M. Segev, A. Szameit, *Nature* **2013**, *496*, 196.
- [32] L. Allen, M. Padgett, M. Babiker, *Prog. Opt.* **1999**, *39*, 291.
- [33] J. A. Davis, D. M. Cottrell, J. Campos, J. Yzuel, I. Moreno, *Appl. Opt.* **1999**, *38*, 5004.
- [34] J. Zhao, P. Zhang, J. B. Zhou, D. X. Yang, D. S. Yang, E. P. Li, *Chin. Phys. Lett.* **2003**, *20*, 1748.
- [35] G. P. Agrawal, *Nonlinear Fiber Optics*, 5th ed., Academic Press, Oxford, UK **2013**.
- [36] F. Diebel, B. M. Bokic, D. V. Timotijevic, D. M. Jovic Savic, C. Denz, *Opt. Express* **2015**, *23*, 24351.
- [37] N. V. Kukhtarev, V. B. Markov, S. G. Odulov, M. S. Soskin, V. L. Vinetskii, *Ferroelectrics* **1979**, *22*, 949.
- [38] A. A. Zozulya, D. Anderson, *Phys. Rev. A* **1995**, *51*, 1520.
- [39] C. Denz, M. Schwab, C. Weilnau, *Transverse-Pattern Formation in Photorefractive Optics*, 1st ed., Springer-Verlag, Berlin, Heidelberg, New York **2003**.

Elliptical vortex necklaces in Mathieu lattices

Jadranka M. Vasiljević,¹ Alessandro Zannotti,² Dejan V. Timotijević,^{1,3} Cornelia Denz,² and Dragana M. Jović Savić¹

¹Institute of Physics, University of Belgrade, P.O. Box 68, 11001 Belgrade, Serbia

²Institut für Angewandte Physik and Center for Nonlinear Science, Westfälische Wilhelms-Universität Münster, 48149 Münster, Germany

³Science Program, Texas A&M University at Qatar, P.O. Box 23874, Doha, Qatar

(Received 25 December 2017; published 27 March 2018)

We demonstrate unusual kinds of discrete vortex beams, elliptical necklaces, realized by Mathieu photonic lattices. Varying the order of the Mathieu lattices and their ellipticity, we can control the shape and size of such necklaces. Besides stable vortex states, we observe oscillatory dipole states or dynamical instabilities and study their orbital angular momentum. Dynamical instabilities occur for higher beam power and higher-order vortices. Also the decay of higher-order phase singularities and their separation is observed in dependence on the ellipticity.

DOI: [10.1103/PhysRevA.97.033848](https://doi.org/10.1103/PhysRevA.97.033848)

I. INTRODUCTION

An optical vortex that possesses a phase singularity and a rotational flow around the singular point in a given direction can be found in physical systems of different nature and scale, ranging from water whirlpools and atmospheric tornadoes to quantized vortices in superfluids and quantized lines of magnetic flux in superconductors [1]. The study of optical vortices and associated localized vortex states is important for both fundamental and applied physics, leading to applications in many areas that include optical data storage, distribution and processing, optical interconnects between electronic chips and boards, and free-space communication links [2–4]. They also have potential uses in optical tweezers [5], optical manipulation and trapping [6,7], microscopy [8], and quantum information processing [9,10].

The evolution of nonlinear excitations in systems whose properties are modulated is especially interesting and in optics can be realized when an intense laser beam propagates in the material with a suitable transverse refractive index modulation that can be fabricated in nonlinear materials including semiconductors, liquid crystals, fused silica, polymers, and photorefractive media [11–18]. The combination of diffractive and nonlinear effects with transverse refractive index modulation in photonic lattices opens the possibility to produce spatially localized states of light [19,20]. To optically induce two-dimensional photonic lattices it is appropriate to use nondiffracting light beams that are exact solutions of the Helmholtz equation in different coordinate systems [21,22]: plane waves in Cartesian, Bessel beams in circular cylindrical [23], Mathieu beams in elliptic cylindrical [24], and parabolic beams in parabolic cylindrical coordinates [25].

In this paper we report on the existence of elliptical necklace beams in photonic lattices optically induced by Mathieu nondiffracting beams, using vortices as a probe beam. These necklace beams show discrete intensity spots on elliptical curves, associated with discrete phase vortices. We investigate the conditions for their existence as well as their properties, both experimentally and theoretically. Changing the lattice ellipticity and choosing Mathieu lattices of appropriate order, we control the shape and the size of an elliptical necklace, as well

as the number of the “pearls” in the necklace. We investigate the breakup of higher-order vortices (topological charge $C_T = 2, 3, 4$) into $C_T = 1$ vortices and their rate of separation during propagation. Phase singularity distances increase with C_T , higher lattice ellipticity, and propagation distance. Further, we study the stability of such elliptic necklaces. Supported by the strong nonlinearity, we show the formation of oscillating dipole states in the intensity distribution for very long propagation distances and discuss our results by investigating additionally the transfer of orbital angular momentum (AM) to the lattice. Finally, a high intensity of the probe beam leads to nonlinear dynamical instabilities observable in the intensity distribution of the necklaces.

II. EXPERIMENTAL METHOD AND MODELING OF VORTEX BEAM PROPAGATION IN MATHIEU LATTICES

Figure 1 shows the experimental setup to realize elliptical necklaces. A frequency-doubled, expanded, and collimated Nd:YVO₄ laser with wavelength $\lambda = 532$ nm is split into two separate beams: an ordinary polarized writing and an extraordinary polarized probe beam. Both are spatially tailored in intensity and phase by a phase-only spatial light modulator Holoeye Pluto VIS. For this purpose, special Fourier filters (FF1 and FF2) are required [26]. The structure beam optically induces refractive index modulations in the 15-mm-long photorefractive Strontium Barium Niobate crystal doped by Cerium (SBN:Ce), thereby addressing the weaker electro-optic coefficient $r_{13} = 47 \text{ pm/V}$. The birefringent crystal has refractive indices $n_o = 2.325$ and $n_e = 2.358$ and is externally biased with an electric field $E_{\text{ext}} = 1600 \text{ V/cm}$ aligned along the optical $c = x$ axis, perpendicular to the direction of propagation (z axis). Probing the artificial photonic structure is done with the extraordinary polarized probe beam that addresses the stronger electro-optic coefficient $r_{33} = 237 \text{ pm/V}$. An imaging system consisting of a microscope objective and camera detects transverse intensity distributions at the back of the crystal.

We model our experiment by solving the nonlinear Schrödinger equation for an initial scalar electric field $A(\mathbf{r})$

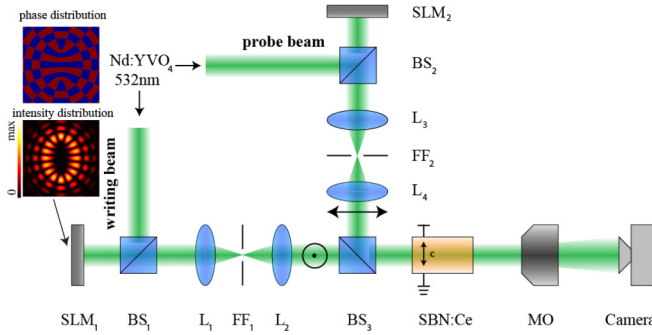


FIG. 1. Experimental setup for the investigation of vortex beams in a Mathieu lattice optically induced in a photorefractive SBN crystal: BS, beam splitter; FF, Fourier filter; L, lens; M, mirror; MO, microscope objective; and SLM, spatial light modulator.

numerically by using a beam propagation method [27]:

$$i\partial_z A(\mathbf{r}) + \frac{1}{2k_z} \Delta_{\perp} A(\mathbf{r}) + \frac{k_z}{2n_{o,e}^2} \delta n^2 [|A(\mathbf{r})|^2] A(\mathbf{r}) = 0. \quad (1)$$

By this, the nonlinear propagation of the field $A(\mathbf{r})$ with longitudinal wave vector k_z in a photorefractive nonlinearity is evaluated. The wave number $k = 2\pi/\lambda = \sqrt{k_{\perp}^2 + k_z^2}$ is defined by the wavelength λ . We use elliptical Laguerre Gaussian vortex beams as probe beams [28]. The potential is given by $\delta n^2 [|A(\mathbf{r})|^2] = -n_{o,e}^4 r_{13,33} E$. The electric field $E = E_{\text{ext}} + E_{\text{sc}}$ that builds up inside the strontium barium niobate (SBN) crystal is a superposition of an external electric field E_{ext} and an internal space charge field E_{sc} that results due to the incident intensity distribution $I(\mathbf{r}) = |A(\mathbf{r})|^2$. Owing to the biased SBN crystal, we use an anisotropic approximation to calculate the refractive index modulation and solve the potential equation [29]

$$\Delta\phi_{\text{sc}} + \nabla\phi_{\text{sc}} \nabla \ln(1 + I + I_{\text{latt}}) = E_{\text{ext}} \partial_x \ln(1 + I + I_{\text{latt}}), \quad (2)$$

where $E_{\text{sc}} = \partial_x \phi_{\text{sc}}$ and I_{latt} is the lattice intensity according to the corresponding Mathieu beams. We use Mathieu beams $M_m(\xi, \eta)$ mathematically described as the product of radial c_{em} and angular J_{em} Mathieu functions of order m ,

$$M_m(\xi, \eta) = C_m(q) J_{\text{em}}(\xi; q) c_{\text{em}}(\eta; q), \quad (3)$$

where $C_m(q)$ is a weighting constant. The functions depend on $q = f^2 k_{\perp}^2 / 4$, a parameter of ellipticity which is related to the positions f of the two foci and the transverse wave number $k_{\perp} = 2\pi/a$, where a is the characteristic structure size; here $I_{\text{latt}} = |M_m(\xi, \eta)|^2$ and $a = 90 \mu\text{m}$. We present results with even Mathieu functions, but our conclusions are the same for odd Mathieu functions.

III. ELLIPTICAL NECKLACE STRUCTURES

To systematically investigate the propagation of vortex beams in Mathieu lattices, we start our studies by considering the Mathieu lattices optically induced with even Mathieu function of order $m = 8$, dependent on different ellipticity parameters q . We examine the conditions of existence of spatially localized vortex states. It is well known that the presence of

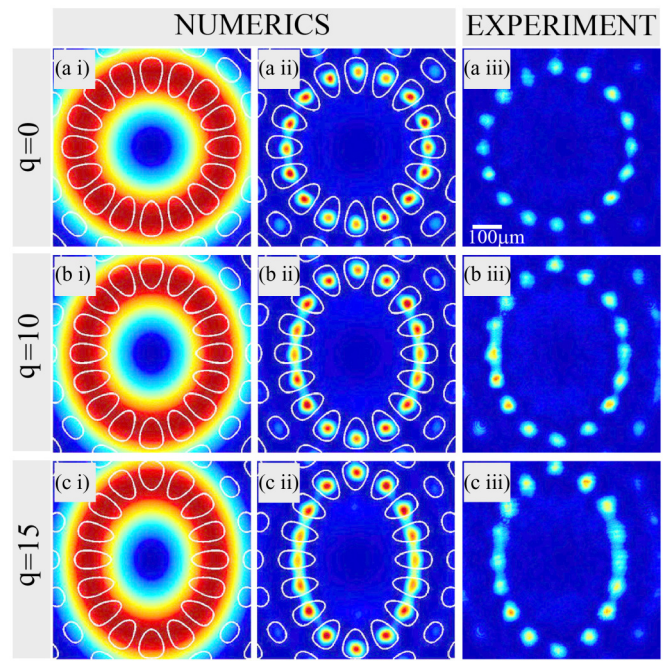


FIG. 2. Elliptical necklaces in Mathieu lattices with different ellipticity parameter q and $C_T = 1$. The input vortex beam is shown with the layout of the lattice beams indicated by open circles (the first column). The corresponding intensity distributions are shown at the exit crystal face in numerics (the second column) and experiment (the third column). The parameters are $E_0 = 1600 \text{ V/cm}$, numerical lattice intensity $I_{\text{latt}} = 0.3$, and input vortex intensity 0.005; the experimental lattice power $P_{\text{latt}} = 20 \mu\text{W}$ and input vortex power 8 μW .

the lattice during vortex breakup induces confinement of the filaments approximately at the location of the incident vortex ring and the surrounding lattice sites. We choose the input vortex beam with $C_T = 1$ to cover the lattice sites of the inner lattice elliptical ring.

Figure 2 summarizes our results for three different values of ellipticity parameter q . At the beginning, we consider the case with no ellipticity ($q = 0$) and observe a stable necklace beam for very low nonlinearity (almost linear). Increasing the lattice ellipticity for the same experimental conditions, we observe elliptical necklaces, with lobes slightly closer to each other, owing to the shape and distribution of the lattice sites in that lattice area. Investigating the stability of these necklaces, we find that these vortex states are stable during propagation along the crystal. With Mathieu lattices of higher order ($m > 8$), we observe elliptical necklaces with a larger number of pearls, staying stable along the length of the crystal. With broader vortex beams we find vortex solutions with two necklaces, covering the inner and next ring of the Mathieu lattice. These states are not stable during the propagation.

Next we investigate higher-order vortex beams in Mathieu lattices. We choose the same input ring vortex beam with different C_T (Fig. 3). Energy flow inside the inner lattice ring causes an increase in asymmetry when incrementing C_T . In the overall phase distribution, we observe a central area having the expected vortex state. However, on the inner lattice ring, we observe a vortex state corresponding to the input C_T , but circularly shifted with respect to the central vortex area.

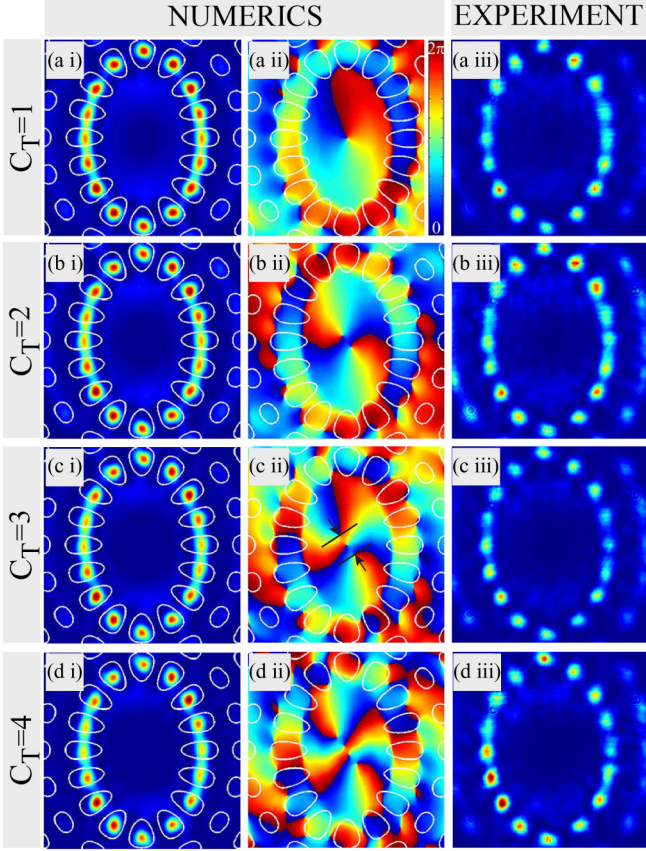


FIG. 3. Single- and multiple-charged elliptical necklaces for the numerically observed intensity (the first column) and phase distributions (the second column). The third column presents experimentally observed intensity distributions. The lattice ellipticity $q = 15$ and other parameters are as in Fig. 2.

Considering phase distributions along the propagation, we observe the phase distribution shifting along the inner lattice ring, as well as in the central part of the phase distributions.

For higher-order vortices we observe a spatial separation of several single-charged phase singularities [30], unlike the conventional multiple-charged vortex where the embedded phase singularity is multiply folded. The elliptical necklaces show an unfolded behavior in the phase distribution, with the

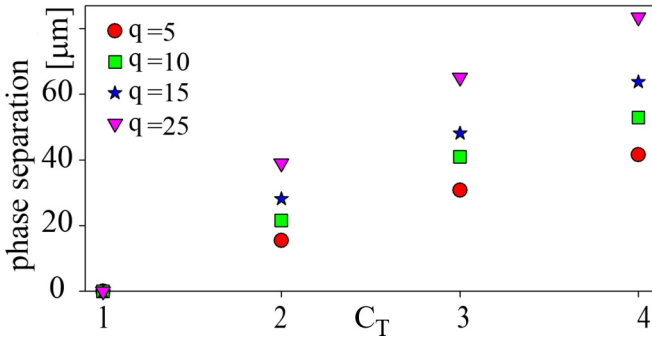


FIG. 4. Phase singularity separation versus C_T for various lattice ellipticities after a 15-mm propagation distance. Separations are measured as the Euclidean distance between the two singularities.

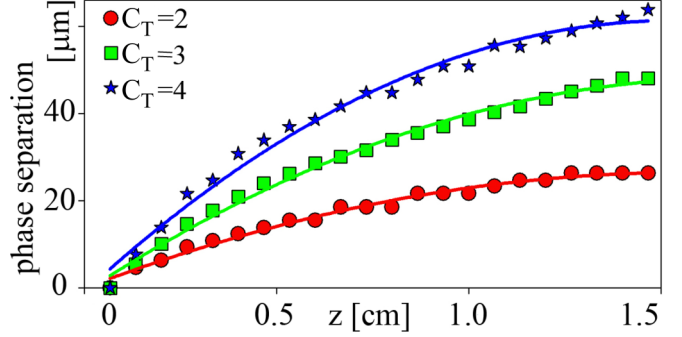


FIG. 5. Phase singularity separation versus propagation distance for various C_T . Separations are measured between the two singularities for lattice ellipticity $q = 15$ as a Euclidean distance. The parameters are as in Fig. 3.

appearance of multiple single-charged phase singularities separated by a finite distance. We found that the phase singularity separation depends on the lattice ellipticity, as well as the input vortex C_T . We measure the Euclidean distance between the two furthest singularities [as indicated in Fig. 3(c ii)] for different lattice ellipticity and presented results in Fig. 4. Higher values of separations are observed for higher ellipticities q . Phase singularity separation distances also increase with propagation distance, for higher $C_T = 2, 3, 4$ and $q = 15$ (Fig. 5). Higher values of separations are observed for higher C_T .

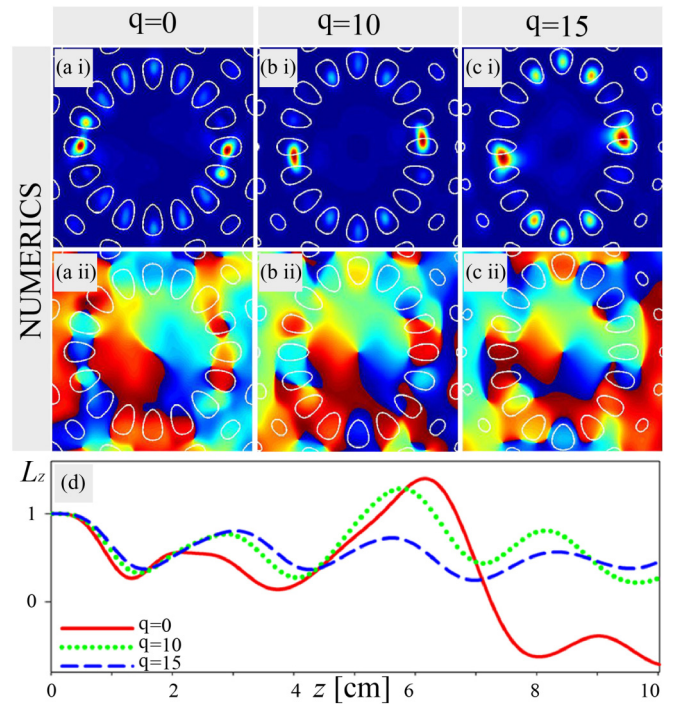


FIG. 6. Dipole states in Mathieu lattices of various ellipticity (a) $q = 0$, (b) $q = 10$, and (c) $q = 15$. Intensity and phase distributions are presented after 10-cm propagation. (d) Normalized z component of the angular momentum along the propagation distance. Other parameters are as in Fig. 2.

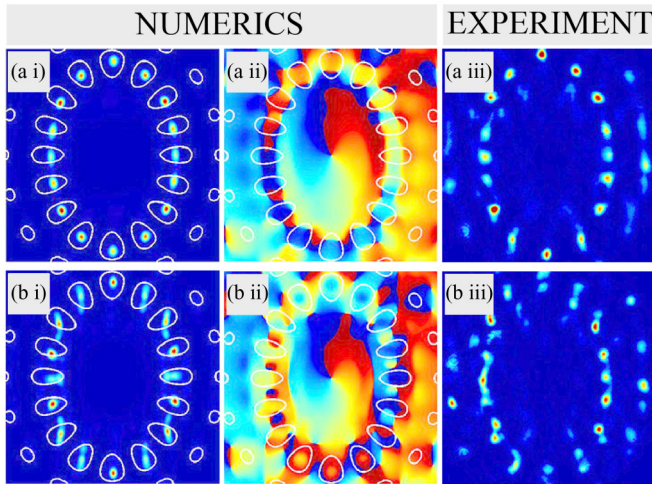


FIG. 7. Nonlinear vortex propagation in Mathieu lattices. The first and third columns present intensity distributions, and the second column presents the corresponding phase distributions at the exit face of crystal. Input vortex intensities in numerics are (a i) 0.01 arb. units and (b i) 0.1 arb. units, and input vortex power in experiment are (a iii) 20 μW and (b iii) 30 μW . The other parameters are as in Fig. 2(c).

IV. ELLIPTICAL NECKLACE INSTABILITIES

Finally, we discuss in detail the (in)stability of elliptical necklaces. We demonstrated in Sec. III that these vortex states observed in linear and very low nonlinear regimes (Fig. 2) are stable during propagation in our nonlinear photorefractive crystal. We also further investigate their stability for longer propagation distances numerically, in order to address length scales that are not accessible in the experiment. While the elliptical necklaces remain stable for propagation length a few times longer than our crystal size, after 10 cm they transforms to oscillating dipole states (Fig. 6). Their phase distributions remain unchanged in the center, but along the inner lattice ring their initial phase distribution for stable states is broken. Higher-order vortex states, observed in the form of slightly asymmetric necklaces [Figs. 3(b)–3(d)] with lower powers, are stable only for short propagation distances (crystal size).

Also, we investigate the orbital AM of necklace beams during propagation [31,32]. The standard definition for the (normalized) z component of the orbital AM is adopted [32]:

$$L_z = -\frac{i}{2} \int \int dx dy A^*(x, y)(x\partial_y - y\partial_x)A(x, y) + \text{c.c.} \quad (4)$$

Figure 6(d) presents the mean orbital AM L_z per transverse plane dependent on the propagation distance z of the necklace states along the propagation distance for different ellipticity parameters q . Less pronounced AM transfer is observed for higher lattice ellipticity. For lower ellipticities, the neighboring lobes exchange more power during the propagation and the transfer of angular momentum from the vortex to the photonic lattice is more pronounced (red plot).

Increasing the input vortex power, we investigate the stability of vortex states. The most illustrative cases are presented in Fig. 7 for vortex states with $C_T = 1$ and lattice ellipticity $q = 15$. With lower powers, neighboring lobes exchange some power, the stable elliptical necklace is broken, and regular oscillations along the propagation take place [Fig. 7(a)]. When increasing the beam power, irregular oscillations take place which are more pronounced for longer propagation distances [Fig. 7(b)]. With higher beam powers, phase distributions stay unchanged only in the central part and are broken along the inner lattice ring.

V. CONCLUSION

In summary, we have demonstrated experimental and numerical investigations of the elliptical necklace in a photorefractive medium with optically induced Mathieu lattices. We have analyzed how various orders of Mathieu lattices and their ellipticities could control the shape and the size of the elliptical necklace, as well as the number of pearls in them. Phase singularity separations were investigated for higher-order vortices. We have observed that such separations increase with C_T , higher lattice ellipticities, and the propagation distance. The stability of elliptical necklaces was studied as well as their AM. Stable vortex states were observed for lower beam powers and shorter distances, but oscillatory dipole states or dynamical instabilities were observed for longer propagation distances, higher beam power, and higher-order vortices. Our results enable further investigations of vortex beam control in photonic lattices optically induced by other than Mathieu beams and could find applications in the field of optical micromanipulation to guide, trap, and sort objects.

ACKNOWLEDGMENTS

This work was supported by the German Academic Exchange Service (Project No. 57219089), the Ministry of Education, Science and Technological Development, Republic of Serbia (Project No. OI 171036), and the Qatar National Research Fund (Grant No. NPRP 7-665-1-125).

-
- [1] L. M. Pismen, *Vortices in Nonlinear Fields* (Clarendon, Oxford, 1999).
 - [2] A. Desyatnykov, Y. Kivshar, and L. Torner, in *Progress in Optics*, edited by E. Wolf (Elsevier, Amsterdam, 2005), Vol. 47, pp. 291–391.
 - [3] J. Wang, *Photon. Res.* **4**, B14 (2016).
 - [4] A. E. Willner, L. L. Guodong Xie, Y. Ren, H. Huang, Y. Yue, N. Ahmed, M. J. Willner, A. J. Willner, Y. Yan, Z. Zhao, Z. Wang, C. Liu, M. Tur, and S. Ashrafi, *Photon. Res.* **4**, B5 (2016).
 - [5] M. J. Padgett and R. Bowman, *Nat. Photonics* **5**, 343 (2011).
 - [6] K. Dholakia and T. Čižmár, *Nat. Photonics* **5**, 335 (2011).
 - [7] L. Paterson, M. P. MacDonald, J. Arlt, W. Sibbett, P. E. Bryant, and K. Dholakia, *Science* **292**, 912 (2001).
 - [8] S. Bernet, A. Jesacher, S. Fürhapter, C. Maurer, and M. Ritsch-Marte, *Opt. Express* **14**, 3792 (2006).
 - [9] A. Mair, A. Vaziri, G. Weihs, and A. Zeilinger, *Nature (London)* **412**, 313 (2001).
 - [10] J. Leach, B. Jack, J. Romero, A. K. Jha, A. M. Yao, S. Franke-Arnold, D. G. Ireland, R. W. Boyd, S. M. Barnett, and M. J. Padgett, *Science* **329**, 662 (2010).

- [11] H. S. Eisenberg, Y. Silberberg, R. Morandotti, A. R. Boyd, and J. S. Aitchison, *Phys. Rev. Lett.* **81**, 3383 (1998).
- [12] D. Mandelik, H. S. Eisenberg, Y. Silberberg, R. Morandotti, and J. S. Aitchison, *Phys. Rev. Lett.* **90**, 053902 (2003).
- [13] T. Pertsch, T. Zentgraf, U. Peschel, A. Brauer, and F. Lederer, *Phys. Rev. Lett.* **88**, 093901 (2002).
- [14] K. A. Brzakiewicz, M. A. Karpierz, A. Fratalocchi, G. Assanto, and E. Nowinowski-Kruszelnicki, *Opto-Electron. Rev.* **13**, 107 (2005).
- [15] F. Chen, M. Stepic, C. E. Rüter, D. Runde, D. Kip, V. Shandarov, O. Manela, and M. Segev, *Opt. Express* **13**, 4314 (2005).
- [16] H. Trompeter, T. Pertsch, F. Lederer, D. Michaelis, U. Stippel, A. Brauer, and U. Peschel, *Phys. Rev. Lett.* **96**, 023901 (2006).
- [17] A. Szameit, D. Blomer, J. Burghoff, T. Schreiber, T. Pertsch, S. Nolte, and A. Tunnerman, *Opt. Express* **13**, 10552 (2005).
- [18] P. Rose, M. Boguslawski, and C. Denz, *New J. Phys.* **14**, 033018 (2012).
- [19] D. N. Christodoulides, F. Lederer, and Y. Silberberg, *Nature (London)* **424**, 817 (2003).
- [20] J. W. Fleischer, M. Segev, N. K. Efremidis, and D. N. Christodoulides, *Nature (London)* **422**, 147 (2003).
- [21] P. Zhang, Y. Hu, T. Li, D. Cannan, X. Yin, R. Morandotti, Z. Chen, and X. Zhang, *Phys. Rev. Lett.* **109**, 193901 (2012).
- [22] E. G. Kalnins and W. Miller, *J. Math. Phys.* **17**, 331 (1976).
- [23] J. Durnin, J. J. Miceli, and J. H. Eberly, *Phys. Rev. Lett.* **58**, 1499 (1987).
- [24] J. C. Gutiérrez-Vega, M. D. Iturbe-Castillo, and S. Chávez-Cerda, *Opt. Lett.* **25**, 1493 (2000).
- [25] M. A. Bandres, J. C. Gutiérrez-Vega, and S. Chávez-Cerda, *Opt. Lett.* **29**, 44 (2004).
- [26] J. A. Davis, D. M. Cottrell, J. Campos, M. J. Yzuel, and I. Moreno, *Appl. Opt.* **38**, 5004 (1999).
- [27] G. Agrawal, *Nonlinear Fiber Optics* (Academic, New York, 2012).
- [28] V. P. Lukin, P. A. Konyaev, and V. A. Sennikov, *Appl. Opt.* **51**, C84 (2012).
- [29] A. A. Zozulya and D. Z. Anderson, *Phys. Rev. A* **51**, 1520 (1995).
- [30] F. Ye, D. Mihalache, and B. Hu, *Phys. Rev. A* **79**, 053852 (2009).
- [31] Z. Chen, H. Martin, A. Bezryadina, D. Neshev, Y. S. Kivshar, and D. N. Christodoulides, *J. Opt. Soc. Am. B* **22**, 1395 (2005).
- [32] M. S. Petrović, D. M. Jović, M. R. Belić, and S. Prvanović, *Phys. Rev. A* **76**, 023820 (2007).

Creating aperiodic photonic structures by synthesized Mathieu-Gauss beams

Jadranka M. Vasiljević,¹ Alessandro Zannotti,² Dejan V. Timotijević,^{1,3} Cornelia Denz,² and Dragana M. Jović Savić¹

¹Institute of Physics, University of Belgrade, P.O. Box 68, 11001 Belgrade, Serbia

²Institut für Angewandte Physik and Center for Nonlinear Science (CeNoS),

Westfälische Wilhelms-Universität Münster, 48149 Münster, Germany

³Science Program, Texas A&M University at Qatar, P.O. Box 23874 Doha, Qatar

(Received 16 May 2017; published 17 August 2017)

We demonstrate a kind of aperiodic photonic structure realized using the interference of multiple Mathieu-Gauss beams. Depending on the beam configurations, their mutual distances, angles of rotation, or phase relations we are able to observe different classes of such aperiodic optically induced refractive index structures. Our experimental approach is based on the optical induction in a single parallel writing process.

DOI: [10.1103/PhysRevA.96.023840](https://doi.org/10.1103/PhysRevA.96.023840)

I. INTRODUCTION

Since nondiffracting beams have been introduced in the late 1980s [1,2] as light structures, only recently these structures have drawn considerable attention in various topics such as trapping of colloidal and *in vivo* particles in biophysics [3], atom optics [4], applications of optical lattices in quantum computing [5], as well as quantum optics [6], optical tweezing [7,8], and nonlinear optics [9–11]. Such nondiffracting structures are coming from the well-known classes of simple nondiffracting light beams that are exact solutions of the Helmholtz equation in different coordinate systems [12]: plane waves in Cartesian, Bessel beams in circular cylindrical [2], Mathieu beams in elliptic cylindrical [13], and parabolic beams in parabolic cylindrical coordinates [14].

A simple and robust implementation of optical micro-manipulation technologies—optical tweezers—based on nondiffracting beams, has become a standard tool in biological, medical, and physics research laboratories [15]. Another trend in optical manipulation is the use of synthesized optical beams rather than single beams only; such beams enable a much greater freedom in object manipulation than conventional Gaussian beams [16].

The potential of nondiffracting structures is of significant importance for advances in discrete and nonlinear modern photonics [17–21]. Although the physics of periodic photonic systems are of fundamental importance, deviations from periodicity are of importance as they may result in higher complexity. One such deviation in optics results in the realization of photonic quasicrystals [20,22], the structures that lie between periodic and disordered one. They show sharp diffraction patterns that confirm the existence of wave interference resulting from their long-range order. Recently, a new serial approach for the generation of aperiodic deterministic Fibonacci and Vogel spirals as refractive index structures was presented [23,24]. In particular, the Fourier spectra of tailored aperiodic lattices can be customized to range from discrete to continuous [25], thus featuring unique light propagation as well as localization properties in aperiodic photonic lattices. Of particular interest are also flat-band lattices with a dispersionless energy band composed of entirely degenerate states, so that any excitation of these states yields nondiffracting waves. Such flat band systems have been studied in a number of lattice models including quasi-one-,

two-, or three-dimensional settings, diamond ladder, Lieb, or kagome lattices [26–28].

In this paper, we demonstrate a powerful approach for the creation of two-dimensional (2D) aperiodic photonic lattices in a single writing process in parallel. It is based on synthesizing two or more nondiffracting Mathieu-Gauss (MG) beams [29]. By coherently superimposing MG beams with different orders, positions, and relative phases we realize transverse invariant propagating intensity distributions capable of optically inducing corresponding refractive index lattices in photosensitive media. Our approach features the fabrication of versatile aperiodic lattices with controllable properties as well as quasi-one-dimensional structures.

II. CHARACTERIZATION OF SYNTHESIZED MATHIEU-GAUSS BEAMS

For the experimental realization of synthesized MG beams we use the experimental setup shown in Fig. 1. We use a frequency-doubled Nd:YVO₄ laser, expand the laser beam, and illuminate as a plane wave a phase-only spatial light modulator “Holoeye Pluto VIS.” The reflected light field is modulated in both amplitude and phase. This is possible by addressing a precalculated hologram to the SLM containing the information of the complex light field encoded with an additional blazed grating. By applying an appropriate Fourier filter, the tailored complex light field is realized [30,31]. Additionally, the telescope L1-L2 scales down the SLM size by a factor of 10. This extraordinary polarized “structure beam” is used to optically inscribe refractive index modulations in the 15 mm long photorefractive SBN:Ce crystal which is externally biased with an electric dc field of $E_{\text{ext}} = 2000 \text{ V cm}^{-1}$ aligned along the optical $c = x$ axis, perpendicular to the direction of propagation (z axis).

We simulate the nonlinear light propagation in a photonic structure by numerically solving the nonlinear Schrödinger equation:

$$i\partial_z A(\mathbf{r}) + \frac{1}{2}\Delta_{\perp} A(\mathbf{r}) + \frac{1}{2}\Gamma E(|A(\mathbf{r})|^2)A(\mathbf{r}) = 0, \quad (1)$$

where $\Gamma = k_0^2 w_0^2 n_{o,e}^4 r_{13,33}$, $k_0 = 2\pi/\lambda$ is the wave number and defined by the wavelength $\lambda = 532 \text{ nm}$, $n_o = 2.325$ is the ordinary, $n_e = 2.358$ is the extraordinary bulk refractive index, $r_{13} = -47 \text{ pm/V}$, $r_{33} = 237 \text{ pm/V}$ are the corresponding

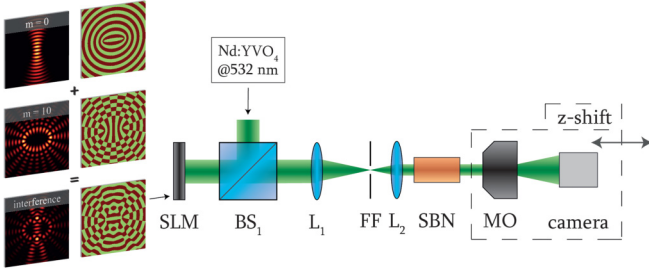


FIG. 1. Experimental setup for the investigation of synthesized MG beams and their optical induction in a photorefractive SBN crystal. BS: beam splitter; FF: Fourier filter; L: lens; MO: microscope objective; SLM: spatial light modulator. Depicted on the left side is a scheme that shows how two single MG beams interfere to create more complex light fields, addressed to the SLM.

electro-optic coefficients, respectively, and w_0 is an arbitrary scaling factor. The electric field $E = E_{\text{ext}} + E_{\text{sc}}$ that builds up inside the SBN crystal is a superposition of an external electric field E_{ext} and an internal space charge field E_{sc} that results due to the incident intensity distribution $I(\mathbf{r}) = |A(\mathbf{r})|^2$. Owing to the biased SBN crystal, we use an anisotropic approximation to calculate the refractive index modulation [32] and solve the potential equation:

$$\Delta\phi_{\text{sc}} + \nabla\phi_{\text{sc}} \cdot \nabla \ln(1+I) = E_{\text{ext}} \partial_x \ln(1+I), \quad (2)$$

where $E_{\text{sc}} = \partial_x \phi_{\text{sc}}$.

The complex aperiodic beams in this work are based on even Mathieu beams $A_m(\xi, \eta)$ [13], mathematically described as a product of radial c_{em} and angular J_{em} Mathieu function of order m :

$$A_m(\xi, \eta) = C_m(q) J_{\text{em}}(\xi; q) c_{\text{em}}(\eta; q), \quad (3)$$

where $C_m(q)$ is a weighting constant that depends on $q = f^2 k_t^2 / 4$, a parameter of ellipticity which is related to the positions f of the two foci and the transverse wave number $k_t = 2\pi/a$, where a is the characteristic structure size. ξ and η are elliptical coordinates and their relation with spatial coordinates x, y are given with $x + iy = f \cosh(\xi + i\eta)$. Here we use $q = 25$ and $a = 25 \mu\text{m}$. Additionally, the Mathieu beams are apodized with Gaussian beams which yields MG beams [29].

We start our investigations by considering the interference of two even MG beams of different order m_1 and m_2 (Fig. 2), and present their intensity distributions at the input crystal face. For MG beams whose orders have the same parity (even or odd), symmetric synthesized MG structures are observed that propagate unchanged as nondiffracting beams due to identical structure sizes of the individual beams. The intensity distributions are presented for two examples in experiment as well as in numerical simulations in Figs. 2(a) and 2(b). We demonstrate that the superposition of two MG beams of different parity leads to asymmetric intensity distributions [Figs. 2(c) and 2(d)]. In the case of the π out of phase interference, mirror symmetric structures are observed (not shown here). For interfering MG beams of different orders and different parities it is possible to observe symmetric structures only for phase differences of $\pi/2$ that are comparable to synthesized mirror symmetric structures.

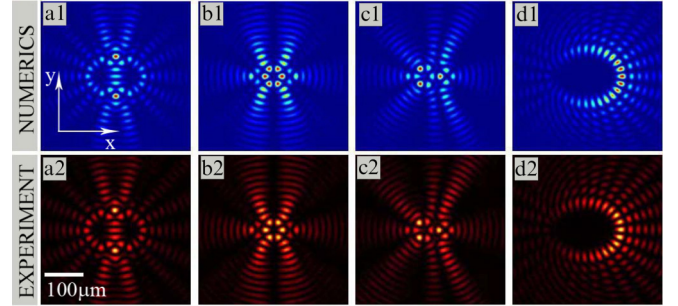


FIG. 2. Interference of two MG beams of different order. Intensity distributions of interfering beams with the same parity: (a) both even: $m_1 = 0, m_2 = 10$; (b) both odd: $m_1 = 1, m_2 = 7$. Intensity distributions of interfering beams with different parity: (c) $m_1 = 2, m_2 = 7$; (d) $m_1 = 13, m_2 = 14$.

Next, we superimpose two even MG beams with the same order, oriented at 90° with respect to each other, considering additionally the in phase and π out of phase configurations. Superimposing MG beams of even parity, we observe distinctive structures for the two different phase configurations [Figs. 3(a), 3(e) and 3(b), 3(f)]. However, using MG beams of odd parity ($m = 5$ or $m = 7$), the same intensity distributions are observed, but mirror symmetric to each other, when changing the phase configurations [Figs. 3(c), 3(g) and 3(d), 3(h)]. This mirror symmetry of superimposed MG beams with odd orders m is related to the intrinsic symmetry of the related Mathieu functions.

Our approach to realize two-dimensional aperiodic lattices finds its origin in synthesizing versatile standard MG beams at different mutual distances. This allows one to continuously increase the degree of aperiodicity. We provide a field

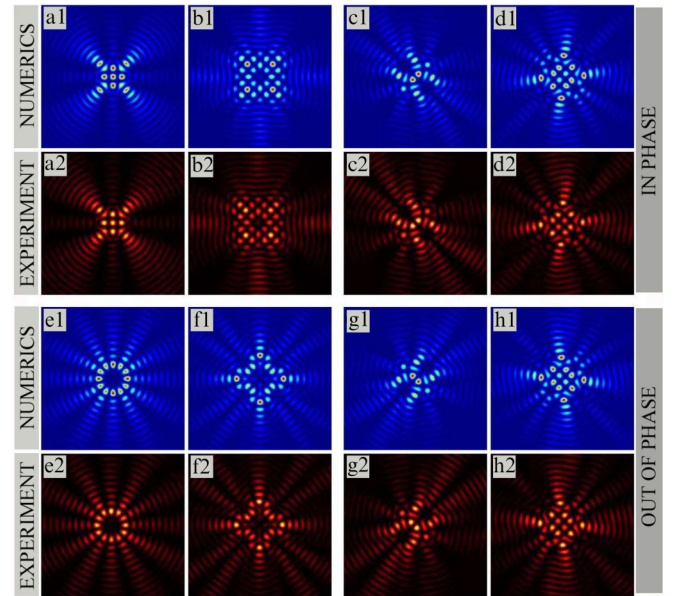


FIG. 3. Transverse interference patterns of two Mathieu-Gauss beams of the same order oriented at 90° with respect to each other: (a),(e) $m_1 = m_2 = 2$, (b),(f) $m_1 = m_2 = 8$ and (c),(g) $m_1 = m_2 = 5$, (d),(h) $m_1 = m_2 = 7$.

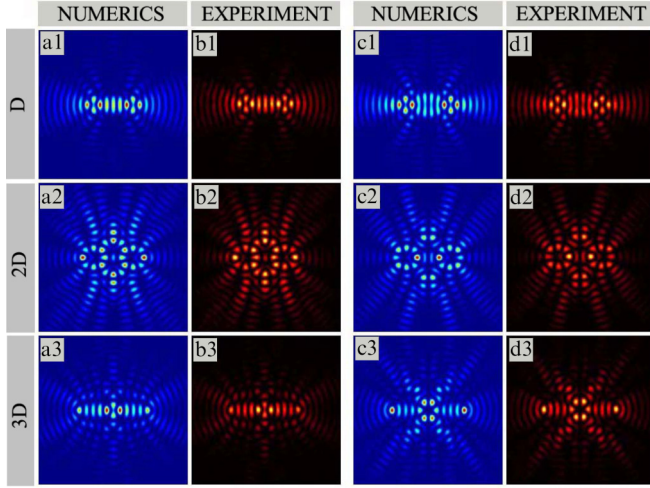


FIG. 4. Interfering MG beams of the same order at different vertical mutual distances: (a),(b) $m = 6$ and (c),(d) $m = 7$. $D = 20 \mu\text{m}$.

distribution that serves as “unit cell” for more complex aperiodic writing light capable of being transferred to tailored refractive index modulations in photosensitive media. A first example that demonstrates the concept (Fig. 4) shows the interference of two even MG beams of the same order. Therefore, we chose MG beams of the order $m = 6$ or $m = 7$ and arrange them at various mutual distances as shown in Figs. 4(a), 4(b) and 4(c), 4(d), respectively. For the following synthesization, we identify the intensity distribution that results for the displacement of $2D = 40 \mu\text{m}$ as most suited.

III. GENERATION OF COMPLEX APERIODIC PHOTONIC STRUCTURES

In order to find conditions for the generation of complex aperiodic photonic structures, we use previously observed synthesized MG beams that provide a unit cell of the photonic lattice. First, we use the example from Fig. 2(b) that has similarities with the unit cell of a periodic lattice created by the interference of six plane waves. By multiplying this structure twice in one row at a distance of $D_x = 80 \mu\text{m}$, we observe a single array [Fig. 5(a)]. Subsequently we multiply the resulting array along the y direction at three different mutual distances $D_y = 80 \mu\text{m}$, $D_y = 88 \mu\text{m}$, and $D_y = 96 \mu\text{m}$. This leads to various aperiodic lattice structures shown in Figs. 5(b)–5(d) that exhibit areas where the initial unit cell is preserving its shape, while additionally novel unit cells emerge whose shape depends on the mutual distances between the multiplied arrays.

Next, configurations are investigated that result from the duplication of the necklace structure from Fig. 3(e). Again, we start with multiplying the structure in one row at different distances. One example is presented in Fig. 5(e) for $D_x = 144 \mu\text{m}$. With such an array, we realize different in two dimensions extended aperiodic structures by changing the mutual distances between the arrays this time additionally in y direction: $D_y = 120 \mu\text{m}$, $D_y = 144 \mu\text{m}$, and $D_y = 152 \mu\text{m}$ [Figs. 5(f)–5(h)]. The initial unit cell is visible in all structures, and it repeats at proper distances, where as well other unit cell

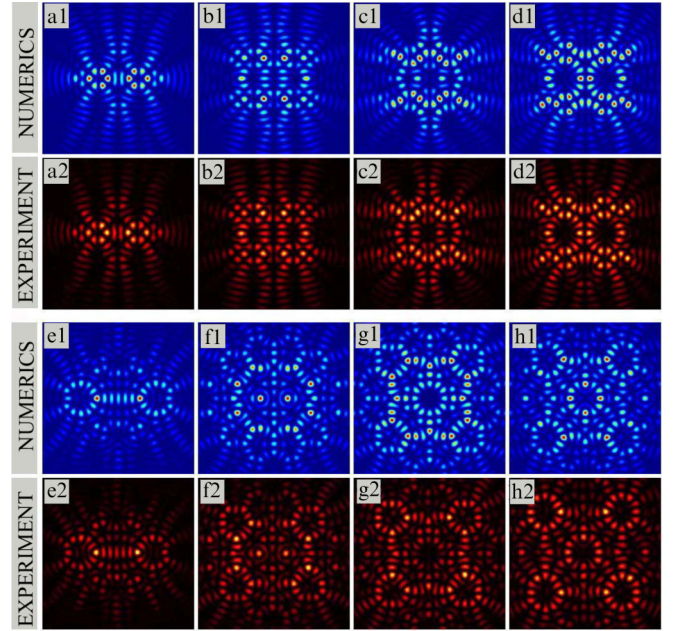


FIG. 5. Generation of aperiodic photonic structures. The first and second rows: multiplying of the structure from Fig. 2(b); the third and fourth rows: multiplying of the structure from Fig. 3(e) at different distances.

structures are visible that can be controlled by changing the distances between initial unit structures used for multiplying.

Figure 6 presents some examples of aperiodic photonic structures, observed using the synthesized MG beams of the sixth and seventh order [Figs. 4(a2) and 4(c2)], as the unit cell. For the synthesized MG beams of the sixth order

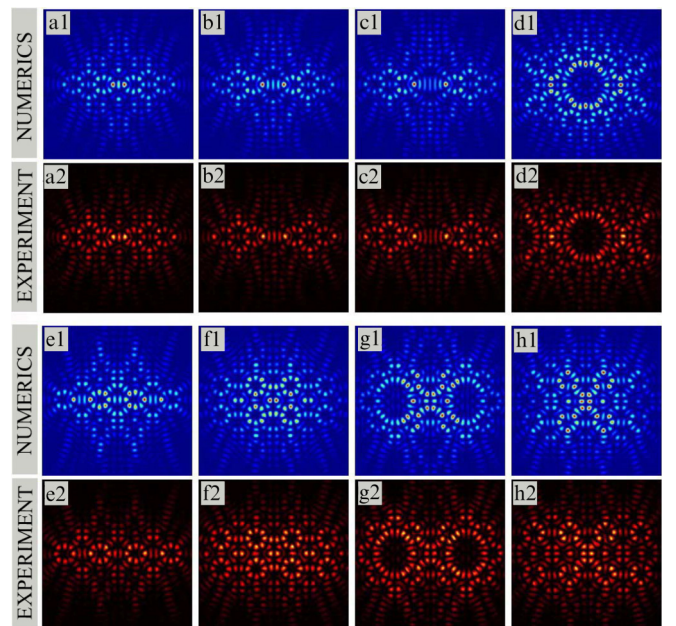


FIG. 6. Aperiodic photonic structures. The first and second row: multiplying of the structure from Fig. 4(a2); the third and fourth row: multiplying of the structure from Fig. 4(c2) at different mutual distances.

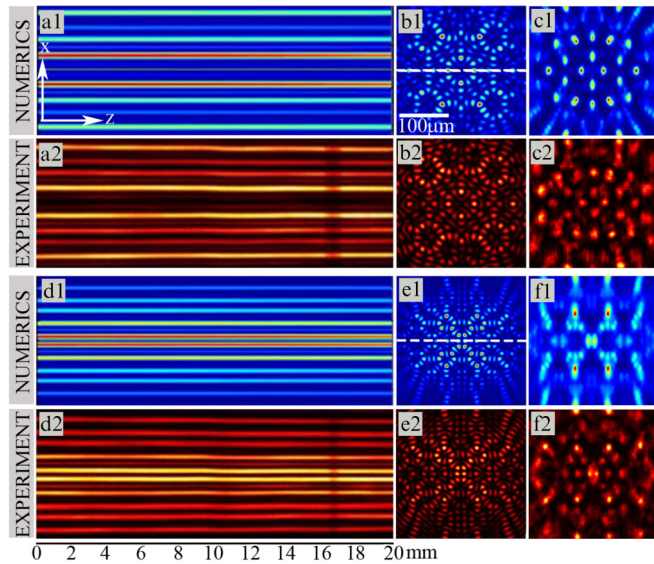


FIG. 7. Waveguiding in aperiodic photonic structures. (a),(b) Lattice beam from Fig. 5(h) and (d),(e) lattice beam from Fig. 6(h) along the longitudinal direction along the propagation, and at the back face of the crystal, respectively. (c),(f) Probe beam at the exit face of the crystal.

(the first and second row), the first three examples present the multiplying of the unit structure along x direction but at different mutual distances: $D_x = 152 \mu\text{m}$ [Fig. 6(a)], $D_x = 176 \mu\text{m}$ [Fig. 6(b)], and $D_x = 192 \mu\text{m}$ [Fig. 6(c)]. As one can see, the shape of the initial structure is preserved, with slightly different interfering patterns between them. The last example [Fig. 6(d)] presents the multiplying of the structure from Fig. 6(b) along y direction for $D_y = 104 \mu\text{m}$.

Synthesized aperiodic MG beams based on seventh order MG beams are presented in the third and fourth row. Figure 6(e) shows the multiplying of the structure from Fig. 4(c2) along the x direction for $D_x = 176 \mu\text{m}$. This structure is further used for multiplying along the y direction at various mutual distances: $D_y = 72 \mu\text{m}$, $D_y = 96 \mu\text{m}$, and $D_y = 104 \mu\text{m}$, and new kinds of aperiodic photonic structures are observed [Figs. 6(f)–6(h)].

We confirm the nondiffracting character of the synthesized MG beams, presented in Figs. 2–6, monitoring their linear propagation through the 20 mm long homogeneous crystal. We exemplarily select the two aperiodic beams demonstrated in Figs. 5(h) and 6(h), and present their linear propagation through the crystal. Figures 7(a) and 7(d) show xz cross sections through the intensity volume that prove

their nondiffracting character. In order to verify that this intensity distribution is capable of realizing aperiodic refractive index modulations, we transfer these ordinary polarized writing beams to aperiodic photonic lattices. The illumination time is 35 s with a moderate laser power of $\approx 30 \mu\text{W}$ and an external electric field of 2000 V/cm. The nonlinear self-interaction is weak and we show the lattice writing beams at the back face of the modulated SBN crystal in Figs. 7(b) and 7(e). Subsequently, we probe the optically induced aperiodic structures with an extraordinarily polarized plane wave. Figures 7(c) and 7(f) conclude these results that clearly demonstrate waveguiding of the initial plane wave in the two-dimensional aperiodic lattice, manifested in a spatially modulated intensity distribution according to the underlying refractive index modulation. Thus the intensity is preferentially guided in areas where the refractive index is increased and spots of high intensity are formed.

The presented method enables the creation of various novel kinds of two-dimensional aperiodic photonic structures in a single optical induction process in parallel. Our approach features the realization of a high versatility of aperiodic lattices that can be tailored in their degree of disorder, ranging from fundamental Mathieu lattices with a high regularity to highly disordered aperiodic structures with quasicontinuous power spectra. It is very flexible owing to the control of the mutual distance between appropriate structures that is easy to realize in experiment, especially compared to previously used optical induction methods [23,24].

IV. CONCLUSIONS

In summary, we have investigated the interference of synthesized MG beams experimentally and numerically. Depending on different configurations, the number of beams, and their mutual distance as well as phase relations, interference effects of two or more spatially displaced or rotated MG beams could be used for optical induction of novel light guiding aperiodic structures in a single parallel writing process. Our experimental results and methods enable further investigations of light propagating in such aperiodic photonic lattices, and could find applications in modern optical information processing.

ACKNOWLEDGMENTS

This work is supported by the German Academic Exchange Service (Project No. 57219089), the Ministry of Education, Science and Technological development, Republic of Serbia (Projects No. OI171036), and the Qatar National Research Fund (NPRP No. 7-665-1-125).

-
- [1] J. Durnin, *J. Opt. Soc. Am. A* **4**, 651 (1987).
 - [2] J. Durnin, J. J. Miceli, and J. H. Eberly, *Phys. Rev. Lett.* **58**, 1499 (1987).
 - [3] D. J. Carnegie, D. J. Stevenson, M. Mazilu, F. Gunn-Moore, and K. Dholakia, *Opt. Express* **16**, 10507 (2008).
 - [4] D. McGloin, G. C. Spalding, H. Melville, W. Sibbett, and K. Dholakia, *Opt. Express* **11**, 158 (2003).
 - [5] R. Raussendorf and H. J. Briegel, *Phys. Rev. Lett.* **86**, 5188 (2001).
 - [6] I. Bloch, *Nat. Phys.* **1**, 23 (2005).
 - [7] V. Garcés-Chávez, D. McGloin, H. Melville, W. Sibbett, and K. Dholakia, *Nature (London)* **419**, 145 (2002).
 - [8] J. Baumgartl, M. Mazilu, and K. Dholakia, *Nat. Photon.* **2**, 675 (2008).

- [9] J. W. Fleischer, M. Segev, N. K. Efremidis, and D. N. Christodoulides, *Nature (London)* **422**, 147 (2003).
- [10] H. Martin, E. D. Eugenieva, Z. Chen, and D. N. Christodoulides, *Phys. Rev. Lett.* **92**, 123902 (2004).
- [11] F. Lederer, G. I. Stegeman, D. N. Christodoulides, G. Assanto, M. Segev, and Y. Silberberg, *Phys. Rep.* **463**, 1 (2008).
- [12] E. G. Kalnins and W. Miller, Jr., *J. Math. Phys.* **17**, 331 (1976).
- [13] J. C. Gutiérrez-Vega, M. D. Iturbe-Castillo, and S. Chávez-Cerda, *Opt. Lett.* **25**, 1493 (2000).
- [14] M. A. Bandres, J. C. Gutiérrez-Vega, and S. Chávez-Cerda, *Opt. Lett.* **29**, 44 (2004).
- [15] M. Woerdemann, C. Alpmann, M. Esseling, and C. Denz, *Laser Photon. Rev.* **7**, 839 (2013).
- [16] C. W. Qiu, D. Palima, A. Novitsky, D. Gao, W. Ding, S. V. Zhukovsky, and J. Gluckstad, *Nanophotonics* **3**, 181 (2014).
- [17] S. Chávez-Cerda, U. Ruiz, V. Arrizón, and H. M. Moya-Cessa, *Opt. Express* **19**, 16448 (2011).
- [18] N. M. Lučić, B. M. Bokić, D. Z. Grujić, D. V. Pantelić, B. M. Jelenković, A. Piper, D. M. Jović, and D. V. Timotijević, *Phys. Rev. A* **88**, 063815 (2013).
- [19] F. Diebel, B. M. Bokić, M. Boguslawski, A. Piper, D. V. Timotijević, D. M. Jović, and C. Denz, *Phys. Rev. A* **90**, 033802 (2014).
- [20] B. Freedman, G. Bartal, M. Segev, R. Lifshitz, D. N. Christodoulides, and J. W. Fleisher, *Nature (London)* **440**, 1166 (2006).
- [21] F. Diebel, B. M. Bokić, D. V. Timotijević, D. M. Jović Savić, and C. Denz, *Opt. Express* **23**, 24351 (2015).
- [22] Z. V. Vardeny, A. Nahata, and A. Agrawal, *Nat. Photon.* **7**, 177 (2013).
- [23] F. Diebel, B. P. Rose, M. Boguslawski, and C. Denz, *Appl. Phys. Lett.* **104**, 191101 (2014).
- [24] M. Boguslawski, N. M. Lučić, F. Diebel, B. D. V. Timotijević, C. Denz, and D. M. Jović Savić, *Optica* **3**, 711 (2016).
- [25] L. D. Negro and S. V. Boriskina, *Laser Photon. Rev.* **6**, 178 (2012).
- [26] D. Leykam, S. Flach, O. Bahat-Treidel, and A. S. Desyatnikov, *Phys. Rev. B* **88**, 224203 (2013).
- [27] J. D. Bodyfelt, D. Leykam, C. Danieli, X. Yu, and S. Flach, *Phys. Rev. Lett.* **113**, 236403 (2014).
- [28] P. P. Beličev, G. Gligorić, A. Radosavljević, A. Maluckov, M. Stepić, R. A. Vicencio, and M. Johansson, *Phys. Rev. E* **92**, 052916 (2015).
- [29] C. López-Mariscal, M. A. Bandres, and J. C. Gutiérrez-Vega, *Opt. Eng.* **45**, 068001 (2006).
- [30] J. A. Davis, D. M. Cottrell, J. Campos, M. J. Yzuel, and I. Moreno, *Appl. Opt.* **38**, 5004 (1999).
- [31] E. Otte, C. Schlickriede, C. Alpmann, and C. Denz, *Proc. SPIE* **9379**, 937908 (2015).
- [32] A. A. Zozulya and D. Z. Anderson, *Phys. Rev. A* **51**, 1520 (1995).

Light propagation in quasi-periodic Fibonacci waveguide arrays

N. M. LUČIĆ, D. M. JOVIĆ SAVIĆ,* A. PIPER, D. Ž. GRUJIĆ, J. M. VASILJEVIĆ,
D. V. PANTELIĆ, B. M. JELENKOVIĆ, AND D. V. TIMOTIJEVIĆ

Institute of Physics, University of Belgrade, P.O. Box 68, 11001 Belgrade, Serbia

*Corresponding author: jovic@jpb.ac.rs

Received 26 March 2015; revised 19 May 2015; accepted 3 June 2015; posted 5 June 2015 (Doc. ID 236998); published 26 June 2015

We investigate light propagation along one-dimensional quasi-periodic Fibonacci waveguide array optically induced in Fe:LiNbO₃ crystal. Two Fibonacci elements, A and B, are used as a separation between waveguides. We demonstrate numerically and experimentally that a beam expansion in such arrays is effectively reduced compared to the periodic ones, without changing beam expansion scaling law. The influence of refractive index variation on the beam expansion in such systems is discussed: more pronounced diffraction suppression is observed for a higher refractive index variation. © 2015 Optical Society of America

OCIS codes: (050.5298) Photonic crystals; (190.5330) Photorefractive optics.

<http://dx.doi.org/10.1364/JOSAB.32.001510>

1. INTRODUCTION

The discovery of quasi-crystals in condensed matter by Shechtman *et al.* [1] and their theoretical analysis by Levine and Steinhardt [2] has inspired a new field of research in optics and photonics.

Examples in the field of optics are photonic quasi-crystals with dielectric multilayers forming the Fibonacci sequence as proposed by Kohmoto *et al.* [3], and realized in [4–6], as well as other deterministic aperiodic structures with long-range order [7,8]. Photonic quasi-crystals have peculiar optical properties. Namely, they lie between periodic and disordered structures and exhibit unique and rich symmetries in Fourier space that are not possible within periodic lattices. The large variety of aperiodic structures is very important and could provide significant flexibility and richness when engineering the optical response of devices [9].

The localization of waves is a ubiquitous phenomenon observed in a variety of classical and quantum systems [10–12], including light waves [13–16], Bose–Einstein condensates [17,18], and sound waves [19]. Although stated more than 50 years ago [11], Anderson localization is still one of the most appealing approaches in optical wave manipulation. In this regard, a transverse localization of light in waveguide lattices turns out to be a particularly interesting concept [13,14]. As the transverse expansion properties in periodic photonic lattices [20–23], as well as in disordered ones [14,24–26], have been investigated extensively, the quasi-periodic photonic lattices emerged as a further attractive research field. The light localization in the Aubry–André model of a quasi-periodic lattice is

observed [27], but the transverse expansion in many other models of photonic quasi-crystals [28] is still an open question.

In this paper, we extend these concepts to the beam expansion in quasi-periodic Fibonacci waveguide arrays, considering light propagation along waveguides. We fabricate the array of identical waveguides (identical refractive index profile). The distance between successive waveguides is modulated in the Fibonacci manner. This means that the sequence of separations consists of two elements, A and B, lined in such a way to make a Fibonacci word. We consider how various input beam positions (incident positions) influence diffraction, and compare them with appropriate periodic waveguide arrays. In general, we find the beam expansion is slowed in quasi-periodic Fibonacci waveguide arrays. Increasing the refractive index variation, the effect is more pronounced.

2. EXPERIMENTAL SETUP AND THEORETICAL BACKGROUND

For the experimental realization of the Fibonacci waveguide array we use LiNbO₃ crystal, doped with 0.05% of iron. Dimensions of the crystal are 3 mm × 0.5 mm × 10 mm, with the optical axis along the *z* direction (10 mm). Waveguides are fabricated using an in-house developed laser writing system with a CW laser at 473 nm and a precise two-axis positioning platform. The platform can move the crystal in the *x*–*z* plane. The laser beam propagates along the *y* axis and it is focused by the 50× microscope objective slightly below the upper surface of the crystal. In this way, the laser makes a controllable local change of the refractive index. By moving the sample along the

z direction, a uniform modification of the refractive index profile is achieved [Fig. 1(a)]. The width of the waveguide obtained in this way is approximately $5 \mu\text{m}$ with a maximum refractive index variation of $\Delta n \sim 1 \times 10^{-4}$, estimated from numerical simulations. The distances between the centers of the adjacent waveguides are $a = 10 \mu\text{m}$ and $b = 16.18 \mu\text{m}$, and follow the Fibonacci word rule, with the golden ratio $b/a = (1 + \sqrt{5})/2$ in our case [Fig. 1(c)].

A scheme of the experimental setup is shown in Fig. 1(b). A beam from He:Ne laser, after appropriate preparation, is focused on the front face of the crystal and propagates along the z direction. The beam waist is around $10.5 \mu\text{m}$ and the power is 10nW . The light is polarized linearly in the y direction. The crystal is situated in a holder which can be moved in the x direction in small steps. In this way, we can launch the beam into appropriate position in the waveguide array. The intensity pattern appearing at the exit face of the crystal is observed by means of an imaging system which consists of a microscope objective and CCD camera.

To theoretically model light propagation in quasi-periodic Fibonacci waveguide arrays, along the propagation distance z , we consider the paraxial wave equation for the slowly varying electric field amplitude E :

$$i \frac{\partial E}{\partial z} = -\frac{1}{2} \frac{\partial^2 E}{\partial x^2} - V(x)E, \quad (1)$$

where $V(x) = n_s + \Delta n \sum_{i=1}^N e^{-(x-x_i)^2/2\sigma^2}$ is the quasi-periodic refractive index profile of the array, n_s is a bulk material refractive index, and Δn is an optically induced refractive index variation. The two Fibonacci elements, A and B, are used as a separation between the waveguides a and b [see Fig. 1(c)]. An array of N waveguides modeled with Gaussian functions centered at x_i is spaced to follow some Fibonacci word. For example, we experimentally realized a waveguide array that represents the following Fibonacci word: ABAABABAABAABABAABA (the first 20 elements) [see

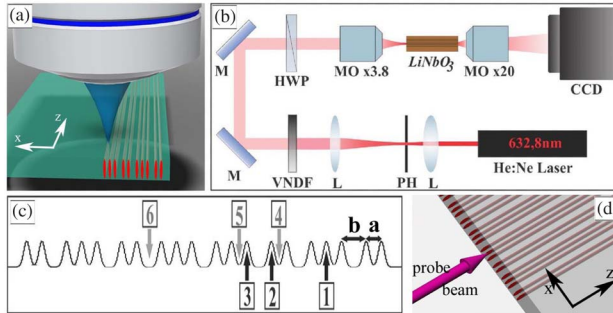


Fig. 1. Setup for an investigation of light propagation in Fibonacci waveguide arrays. (a) Scheme of the laser writing waveguide arrays process in an Fe:LiNbO₃ crystal. (b) Schematic of the experimental setup: He:Ne laser at 632.8 nm; L, lens; PH, pinhole; VNDF, variable neutral density filter; M, mirror; HWP, half-wave plate; MO, microscope objective; CCD, camera. (c) A schematic of a refractive index profile used in numerics ($V(x)$), with two separations between waveguides, a and b . Arrows with numbers show incident beam positions inside waveguides (black) and between waveguides (gray). (d) Schematic geometry of Fibonacci lattice with Gaussian probe beam.

Fig. 1(c)]. For solving our model equation, we use the split-step method with the parameters of our experiment.

3. LIGHT PROPAGATION IN FIBONACCI WAVEGUIDE ARRAYS: EXPERIMENT VERSUS THEORY

We consider beam propagating in Fibonacci waveguide arrays fabricated in our crystal, launched at different incident positions. The propagation characteristics are obtained numerically and experimentally; Fig. 2 summarizes our results. We choose three typical incident positions *inside* waveguides marked by numbers 1, 2, and 3 in Fig. 1(c). Propagations from these positions are represented in the first, second, and third row in Fig. 2. The first column presents intensity distribution along the propagation distance observed numerically, with output profiles in the second column. Experimental results for the same incident positions are presented as intensity distributions at the exit face of the crystal (the forth column) with corresponding profiles in the third column. One can see a very good agreement with numerically obtained profiles.

The main reason for more pronounced diffraction suppression for incident beam positions 1 and 2 [Figs. 2(b) and 2(f)], in comparison with position 3 [Fig. 2(j)], is the separation between incident and neighboring waveguides. While propagating in the medium, the beam displays slowing of beam expansion, compared to the appropriate periodic waveguide arrays [Fig. 4(b)].

Next, we study beam propagating characteristics for incident positions *between* waveguides marked by numbers 4, 5, and 6 in Fig. 1(c). Figure 3 summarizes our numerical and experimental results for these cases. The layout of this figure is the same as in Fig. 2: incident positions 4, 5, and 6 in Fig. 1(c) correspond to the results in the first, second, and third row in Fig. 3, respectively. Beam diffraction for incident positions

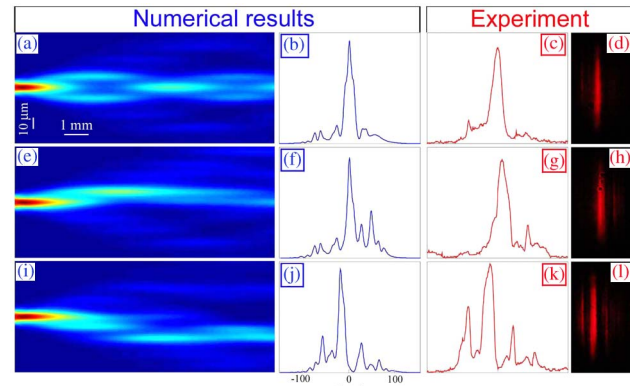


Fig. 2. Light propagation in Fibonacci waveguide arrays. Incident positions of the beam are *inside* certain waveguides, marked with numbers in Fig. 1(c): the first row corresponds to the position 1; the second row corresponds to 2; and the third row corresponds to 3. Intensity distributions of the beam in longitudinal direction during the propagation: (a), (e), and (i) observed numerically. Corresponding intensity profiles at the exit face of the crystal observed numerically: (b), (f), and (j) and experimentally (c), (g), and (k). Experimentally measured intensity distributions at the exit face of the crystal (d), (h), and (l). Physical parameters: the crystal length $L = 1 \text{ cm}$, refractive index variation $\Delta n = 1 \times 10^{-4}$, and Gaussian beam width $10 \mu\text{m}$.

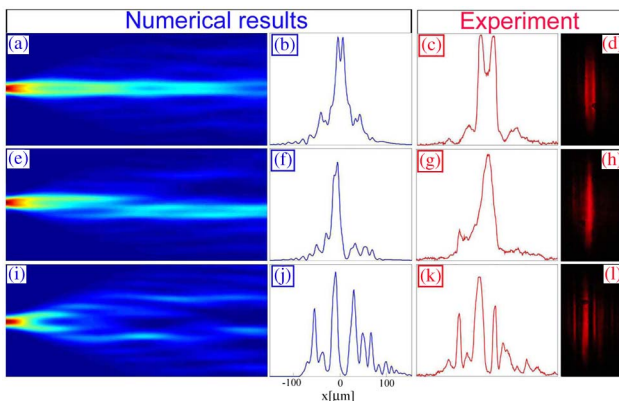


Fig. 3. Light propagation in Fibonacci waveguide arrays with incident positions of the beam *between* certain waveguides, marked with numbers in Fig. 1(c): position 4 corresponds to the first row, 5 to the second row, and 6 to the third row. Intensity distributions of the beam in longitudinal direction during the propagation: (a), (e), and (i) observed numerically. Corresponding intensity profiles at the exit face of the crystal observed numerically (b), (f), and (j) and experimentally (c), (g), and (k). Experimentally measured intensity distributions at the exit face of the crystal (d), (h), and (l). Physical parameters are as in Fig. 2.

between waveguides is more pronounced than for incident positions *inside* waveguides (Fig. 2), but again less pronounced than in periodic waveguide arrays [Fig. 4(b)]. One can see a more pronounced tendency toward diffraction suppression for incident beam position 5 [Fig. 3(g)], compared with 4 [Fig. 3(c)] and 6 [Fig. 3(k)]. We want to stress that these conclusions are relevant only for the distance of propagation in our experiment (1 cm). More general conclusions are drawn in the next chapter, where numerical simulations are performed on longer propagation distances.

4. LIGHT PROPAGATION IN WAVEGUIDE ARRAYS: PERIODIC VERSUS FIBONACCI

We study numerically the beam propagation in Fibonacci waveguide arrays considering longer propagation distances ($L = 10$ cm). To characterize the level of beam expansion, we use the effective beam width $\omega_{\text{eff}} = P^{-1/2}$, where $P = \int |E|^4(x, L) dx / \{\int |E|^2(x, L) dx\}^2$ is the inverse participation ratio. In such a system, it is useful to perform averaging over different incident beam positions to remove the effects of the local environment, i.e., the influence of the neighboring waveguides. Averaged effective beam width is calculated along the propagation distance, and compared for the Fibonacci waveguide array and three different periodic waveguide arrays. Separations a and b in Fibonacci waveguide arrays are used as periods $d = 16.18 \mu\text{m}$ and $d = 10 \mu\text{m}$ for two periodic waveguide arrays. The third periodic array is produced in such a way that the same number of waveguides as in quasi-periodic is arranged in periodic manner in the same space (in our geometry, its lattice period is $d = 12.38 \mu\text{m}$), aimed as the most appropriate for comparison with Fibonacci waveguide array.

Figure 4(a) presents the averaged effective width (averaged over incident positions) along the propagation distance for Fibonacci lattice and refractive index variation $\Delta n = 1 \times 10^{-4}$,

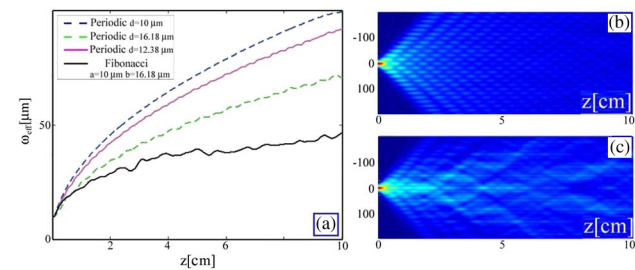


Fig. 4. Comparison between beam diffraction in periodic and quasi-periodic waveguide arrays. (a) Averaged effective beam widths versus the propagation distance, for refractive index variation $\Delta n = 1 \times 10^{-4}$. (b) Field intensity of the beam in longitudinal direction (z) during the propagation for periodic lattice with $d = 12.38 \mu\text{m}$. (c) Averaged field intensity distribution for Fibonacci lattice. Crystal length is $L = 10$ cm.

with the effective beam width for all previously mentioned periodic lattices for the same value of refractive index variation. It should be stressed that the beam width increases more slowly in a Fibonacci lattice compared to the periodic lattices. Clearly, the beam propagation in periodic lattice with $d = 10 \mu\text{m}$ displays the strongest discrete diffraction, followed by other periodic lattices and then quasi-periodic. We also observe that the Fibonacci lattice follows the same beam expansion scaling law [29]. For shorter propagation distances (up to 1.5 cm), beam diffraction in the periodic lattice with $d = 16.18 \mu\text{m}$ is slightly less pronounced than in quasi-periodic because of the weaker coupling between adjacent waveguides in that lattice.

Figure 4(b) presents a typical beam spreading along the propagation distance, for a periodic lattice with $d = 12.38 \mu\text{m}$, simulated for 10 cm of propagation. The averaged intensity distribution for hundreds of different incident positions in a Fibonacci lattice is presented in Fig. 4(c). Compared with the appropriate periodic lattice [Fig. 4(b)], a tendency of Fibonacci lattice to suppress diffraction is evident [Fig. 4(c)].

5. DEPENDENCE OF LIGHT PROPAGATION ON THE REFRACTIVE INDEX VARIATION

At the end, we study the influence of various refractive index variations (Δn) on the beam propagation in Fibonacci waveguide arrays. Again, we calculate the averaged effective width along the propagation distance for each value of Δn . The increase of refractive index variation makes diffraction suppression more pronounced [Fig. 5(a)]: the broadening of the beam becomes almost completely suppressed for longer propagation distances. These curves show a transition from ballistic spreading (normal diffusion) to anomalous diffusion. In addition, a higher refractive index variation changes the anomalous diffusion behavior. The averaged intensity distribution, for hundreds of different incident positions, is presented for $\Delta n = 2 \times 10^{-4}$ in Fig. 5(b), and $\Delta n = 4 \times 10^{-4}$ in Fig. 5(c). These should be compared with the corresponding distribution in Fig. 4(c) for $\Delta n = 1 \times 10^{-4}$. The tendency to suppress diffraction is evident as for a higher refractive index variation; a larger portion of the beam is confined between adjacent waveguides.

Typical averaged intensity distribution profiles in longitudinal direction for propagation lengths of 2, 3, and 4 cm are presented

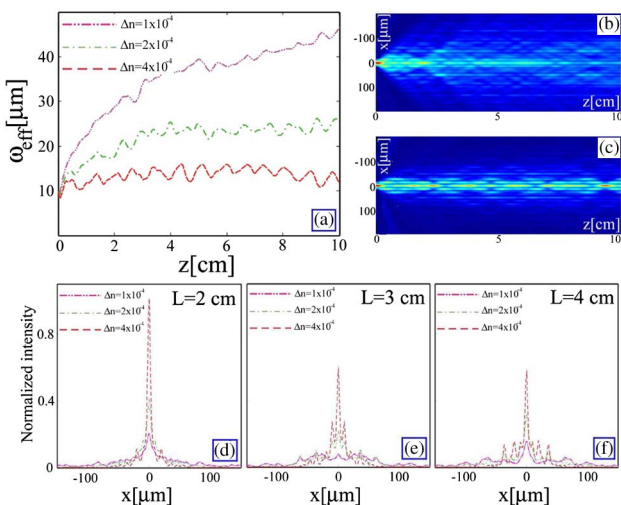


Fig. 5. Light propagation in Fibonacci lattice for a higher refractive index variation. (a) Comparison between propagation in waveguide arrays with different refractive index variation: averaged effective beam widths versus the propagation distance. Averaged field intensity distributions for (b) $\Delta n = 2 \times 10^{-4}$ and (c) $\Delta n = 4 \times 10^{-4}$. Intensity distribution profiles for the same values of Δn at different propagation distances: (d) 2 cm, (e) 3 cm, and (f) 4 cm.

for three values of refractive index variation: $\Delta n = 1 \times 10^{-4}$, $\Delta n = 2 \times 10^{-4}$, and $\Delta n = 4 \times 10^{-4}$ [Figs. 5(d)–5(f)]. Again, one can see a transition toward stronger diffraction suppression with a higher refractive index variation.

6. CONCLUSIONS

In summary, we have observed the beam expansion is slowed down in optically induced Fibonacci waveguide arrays. We have analyzed experimentally and numerically how various incident positions influence propagation characteristics. The experimental results fully agree with the theoretical analysis. Diffraction suppression is observed with Fibonacci waveguide arrays, compared to the appropriate periodic waveguide arrays. We have investigated the influence of refractive index variation on the beam spreading in Fibonacci waveguide arrays. More pronounced diffraction suppression is observed for higher refractive index variations.

Funding. Ministry of Education, Science and Technological Development, Republic of Serbia (OI 171036, OI 171038, III 45016).

REFERENCES

- D. Shechtman, I. Blech, D. Gratias, and J. W. Cahn, "Metallic phase with long-range orientational order and no translational symmetry," *Phys. Rev. Lett.* **53**, 1951–1953 (1984).
- D. Levine and P. J. Steinhardt, "Quasicrystals: a new class of ordered structures," *Phys. Rev. Lett.* **53**, 2477–2480 (1984).
- M. Kohmoto, B. Sutherland, and K. Iguchi, "Localization in optics: quasiperiodic media," *Phys. Rev. Lett.* **58**, 2436–2438 (1987).
- G. Gumbs and M. K. Ali, "Dynamical maps, Cantor spectra, and localization for Fibonacci and related quasiperiodic lattices," *Phys. Rev. Lett.* **60**, 1081–1084 (1988).
- W. Gellermann, M. Kohmoto, B. Sutherland, and P. C. Taylor, "Localization of light waves in Fibonacci dielectric multilayers," *Phys. Rev. Lett.* **72**, 633–636 (1994).
- L. D. Negro, C. J. Oton, Z. Gaburro, L. Pavesi, P. Johnson, A. Lagendijk, R. Righini, M. Collocci, and D. S. Wiersma, "Light transport through the band-edge states of Fibonacci quasicrystals," *Phys. Rev. Lett.* **90**, 055501 (2003).
- W. Steurer and D. Suter-Widmer, "Photonic and phononic quasicrystals," *J. Phys. D* **40**, R229–R247 (2007).
- E. L. Albuquerque and M. G. Cottam, "Theory of elementary excitations in quasiperiodic structures," *Phys. Rep.* **376**, 225–337 (2003).
- Z. V. Vardeny, A. Nahata, and A. Agrawal, "Optics of photonic quasicrystals," *Nat. Photonics* **7**, 177–187 (2013).
- P. Sheng, *Scattering and Localization of Classical Waves in Random Media* (World Scientific, 1990).
- A. Lagendijk, B. Tiggelen, and D. S. Wiersma, "Fifty years of Anderson localization," *Phys. Today* **62**(8), 24–29 (2009).
- S. S. Abdullaev and F. Kh. Abdullaev, "On the light propagation in the system of tunnel-coupled waveguides," *Sov. J. Radiofizika* **23**, 766 (1980).
- T. Pertsch, U. Peschel, J. Kobelke, K. Schuster, H. Bartelt, S. Nolte, A. Tunnermann, and F. Lederer, "Nonlinearity and disorder in fiber arrays," *Phys. Rev. Lett.* **93**, 053901 (2004).
- T. Schwartz, G. Bartal, S. Fishman, and M. Segev, "Transport and Anderson localization in disordered two-dimensional photonic lattices," *Nature* **446**, 52–55 (2007).
- S. Gentilini, A. Fratalocchi, L. Angelani, G. Ruocco, and C. Conti, "Ultrashort pulse propagation and the Anderson localization," *Opt. Lett.* **34**, 130 (2009).
- C. Conti and A. Fratalocchi, "Dynamic light diffusion, three-dimensional Anderson localization and lasing in inverted opals," *Nat. Phys.* **4**, 794–798 (2008).
- G. Roati, C. D'Errico, L. Fallani, M. Fattori, C. Fort, M. Zaccanti, G. Modugno, M. Modugno, and M. Inguscio, "Anderson localization of a non-interacting Bose-Einstein condensate," *Nature* **453**, 895–898 (2008).
- J. Billy, V. Josse, Z. Zuo, A. Bernard, B. Hambrecht, P. Lagan, D. Clément, L. Sanchez-Palencia, P. Bouyer, and A. Aspect, "Direct observation of Anderson localization of matter waves in a controlled disorder," *Nature* **453**, 891–894 (2008).
- J. D. Maynard, "Acoustical analogs of condensed-matter problems," *Rev. Mod. Phys.* **73**, 401–417 (2001).
- H. S. Eisenberg, Y. Silberberg, R. Morandotti, and J. S. Aitchison, "Diffraction management," *Phys. Rev. Lett.* **85**, 1863–1866 (2000).
- T. Pertsch, T. Zentgraf, U. Peschel, A. Bräuer, and F. Lederer, "Anomalous refraction and diffraction in discrete optical systems," *Phys. Rev. Lett.* **88**, 093901 (2002).
- D. N. Christodoulides, F. Lederer, and Y. Silberberg, "Discretizing light behavior in linear and nonlinear waveguide lattices," *Nature* **424**, 817–823 (2003).
- A. Fratalocchi and G. Assanto, "Light propagation through a nonlinear defect: symmetry breaking and controlled soliton emission," *Opt. Lett.* **31**, 1489–1491 (2006).
- D. M. Jović, Yu. S. Kivshar, C. Denz, and M. R. Belić, "Anderson localization of light near boundaries of disordered photonic lattices," *Phys. Rev. A* **83**, 033813 (2011).
- D. M. Jović, M. R. Belić, and C. Denz, "Transverse localization of light in nonlinear photonic lattices with dimensionality crossover," *Phys. Rev. A* **84**, 043811 (2011).
- Y. Lahini, A. Avidan, F. Pozzi, M. Sorel, R. Morandotti, D. N. Christodoulides, and Y. Silberberg, "Anderson localization and nonlinearity in one-dimensional disordered photonic lattices," *Phys. Rev. Lett.* **100**, 013906 (2008).
- Y. Lahini, R. Pugatch, F. Pozzi, M. Sorel, R. Morandotti, N. Davidson, and Y. Silberberg, "Observation of a localization transition in quasi-periodic photonic lattices," *Phys. Rev. Lett.* **103**, 013901 (2009).
- E. Maciá, "The role of aperiodic order in science and technology," *Rep. Prog. Phys.* **69**, 397–441 (2006).
- S. Longhi, "Discrete diffraction and shape-invariant beams in optical waveguide arrays," *Phys. Rev. A* **79**, 033847 (2009).

- Studies on coupling between guided modes and tamm states in one-dimensional photonic crystals**, Sudha Maria Lis S., Shivakiran N. B. Bhaktha, Pratyusha Das, Sakshi Sharma, Indian Institute of Technology Kharagpur (India) [10672-124]
- Enhanced graphene nonlinear response through geometrical plasmon focusing**, Jose Ramón Martínez Saavedra, ICFO - Institut de Ciències Fotòniques (Spain); F. Javier García de Abajo, ICFO - Institut de Ciències Fotòniques (Spain) and Institució Catalana de Recerca i Estudis Avançats (Spain) [10672-125]
- Waveguide-integrated narrowband transmission filter consisting of two grooves and a ridge cavity**, Evgeni A. Bezus, Leonid L. Doskolovich, Dmitry A. Bykov, Image Processing Systems Institute, Russian Academy of Sciences (Russian Federation) [10672-126]
- Efficient synthesis and optical properties of highly luminescent copper nanoclusters**, Maria Jessabel Talite, National Chiao Tung Univ. (Taiwan); Chi-Tsu Yuan, Chung Yuan Christian Univ. (Taiwan); Wu-Ching Chou, National Chiao Tung Univ. (Taiwan) [10672-127]
- Numerically optimized design for enhanced coupling efficiency of single-photon sources integrated into single-mode waveguides**, Theresa Hoehne, Zuse Institute Berlin (Germany); Peter Schnauber, Sven Rodt, Stephan Reitzenstein, Institut für Festkörperphysik, Technische Univ. Berlin (Germany); Sven Burger, Zuse Institute Berlin (Germany) and JCMwave GmbH (Germany) [10672-128]
- Dielectro-plasmonic tweezers for scalable trapping and hot electrons applications**, Alberto Lauri, Emiliano Cortés, Evangelina Pensa, Imperial College London (United Kingdom); Avijit Barik, Univ. of Minnesota (United States); Aliaksandra Rakovich, Imperial College London (United Kingdom); Sang-Hyun Oh, Univ. of Minnesota (United States); Stefan A. Maier, Imperial College London (United Kingdom) [10672-129]
- Surface wave detection of hypersound in single plasmonic nanoantennas**, Rodrigo Berte, Imperial College London (United Kingdom); Fabricio Della Picca, Lab. de Electronica Cuantica, Univ. de Buenos Aires (Argentina) and El Instituto de Física de Buenos Aires (Argentina) and Consejo Nacional de Investigaciones Científicas y Técnicas (Argentina); Yi Li, Emiliano Cortés, Imperial College London (United Kingdom); Stefan A. Maier, Imperial College London (United Kingdom) and Ludwig-Maximilians-Univ. München (Germany); Andrea Braga, Lab. de Electronica Cuantica, Univ. de Buenos Aires (Argentina) [10672-130]
- Anderson localization of visible light for high-quality on-chip optical cavities**, Oliver Trojak, Tom Crane, Luca Sapienza, Univ. of Southampton (United Kingdom) [10672-131]
- Polarization conversion within ultracompact on-chip all-plasmonic nanocircuits**, Martin Thomaszewski, Yuanqing Yang, Sergey I. Bozhevolnyi, Univ. of Southern Denmark (Denmark) [10672-132]
- Optical sensing with Anderson localized light**, Oliver Trojak, Tom Crane, Luca Sapienza, Univ. of Southampton (United Kingdom) [10672-133]
- Plasmon-exciton interaction in the thin film of inhomogeneous ensemble of silver nanoparticles and cyanine J-aggregates**, Anton A. Starovoytov, Rezida D. Nabiullina, Igor A. Gladskih, ITMO Univ. (Russian Federation) [10672-134]
- Planar waveguide coupler based on tilted Bragg gratings and a discrete cladding mode**, Mathias Weisen, Matthieu T. Posner, Optoelectronics Research Ctr. (United Kingdom); James C. Gates, Optoelectronics Research Ctr., Univ. of Southampton (United Kingdom); Corin Gawith, Peter G. R. Smith, Peter Horak, Optoelectronics Research Ctr. (United Kingdom) [10672-135]
- Investigation of bimetallic hollow nanoparticles for colorimetric detection of mercury**, Sangeeta Yadav, VIT Univ. (India); Saumey Jain, KTH Royal Institute of Technology (Sweden); Jitendra Satija, Ctr. for Nanobiotechnology, VIT Univ. (India) [10672-136]
- Using all dielectric and plasmonic cross grating metasurface for enhancing efficiency of CZTS solar cells**, Omar A. M. Abdelaouf, The American Univ. in Cairo (Egypt) and Ain Shams Univ. (Egypt); Ahmed Shaker, Ain Shams Univ. (Egypt); Nageh K. Allam, The American Univ. in Cairo (Egypt) [10672-137]
- Study of thermo-optical properties of nanofluids of gold and silver nanoparticles functionalized with polyethylene glycol and sodium dodecyl sulfate in water using thermal lens spectroscopy**, Orlando Villegas, Jimmy Castillo, Alberto Fernández, Hector Gutierrez, Univ. Central de Venezuela (Venezuela) [10672-138]
- One-pot synthesis red emission of photoluminescent silane capped gold nanoclusters**, Hsiu-Ying Huang, Chi-Tsu Yuan, Chung Yuan Christian Univ. (Taiwan) [10672-139]
- Nanofabrication on unconventional platforms: implications for novel opto-electronic functionalities, design, and enhanced performance**, Jagdish Anakkavoor Krishnaswamy, Kavita Garg, Sandeep B.S., Kumar M.P., Praveen C. Ramamurthy, Debiprosad Roy Mahapatra, Indian Institute of Science (India) [10672-140]
- The glutathione-capped gold nanoclusters based on doping zinc ion with aggregation-induced emission enhancement**, Kun-Blin Cai, Li-Yun Chang, Chi-Tsu Yuan, Hsiu-Ying Huang, Chung Yuan Christian Univ. (Taiwan) [10672-141]
- Near-field localization of Au nano-objects: PEEM and group theory description**, Sarra Mitiche, Sylvie Marguet, Fabrice Charra, Ludovic Douillard, CEA-Ctr. de SACLAY (France) [10672-142]
- Nanostructured layer of InP on GaP surface**, Tinatin Laperashvili, Orest Kvitsiani, Institute of Cybernetics (Georgia); Davit Lapherashvili, Georgian Technical Univ. (Georgia) [10672-143]
- Integration of carbon nanotubes in slot photonic crystal cavities**, Elena Durán-Valdeiglesias, Ctr. de Nanosciences et de Nanotechnologies (France); Thi Hong Cam Hoang, Ctr. de Nanosciences et de Nanotechnologies (France) and Institute of Materials Science (Viet Nam); Carlos Alonso-Ramos, Samuel Serna, Ctr. de Nanosciences et de Nanotechnologies (France); Weiwei Zhang, Ctr. de Nanosciences et de Nanotechnologies (France) and Univ. of Southampton (United Kingdom); Xavier Le Roux, Ctr. de Nanosciences et de Nanotechnologies (France); Matteo Balestrieri, CEA-Ctr. de SACLAY (France) and Commissariat à l'Énergie Atomique (France) and Nanosciences et Innovation pour les Matériaux, la Biomédecine et l'Énergie (France); Francesco Biccaro, Anna Vinattieri, Lab. Europeo di Spettroscopia Non-Lineare, Univ. degli Studi di Firenze (Italy); Delphine Marris-Morini, Ctr. de Nanosciences et de Nanotechnologies (France); Arianna Filoromo, CEA-Ctr. de SACLAY (France) and Commissariat à l'Énergie Atomique (France) and Nanosciences et Innovation pour les Matériaux, la Biomédecine et l'Énergie (France); Massimo Gurioli, Lab. Europeo di Spettroscopia Non-Lineare, Univ. degli Studi di Firenze (Italy); Eric Cassan, Ctr. de Nanosciences et de Nanotechnologies (France) [10672-144]
- Optical coupling of a Mie-resonant silicon nanoparticle to a waveguide revealed by third harmonic generation spectroscopy**, Kirill I. Okhlopkov, Alexander A. Ezhev, Pavel A. Shafirin, M.V. Lomonosov Moscow State Univ. (Russian Federation); Nikolay A. Orlikovskiy, Bauman Moscow State Technical Univ. (Russian Federation); Maxim R. Shcherbakov, M.V. Lomonosov Moscow State Univ. (Russian Federation) and Cornell Univ. (United States); Andrey A. Fedyanin, M.V. Lomonosov Moscow State Univ. (Russian Federation) [10672-145]
- Distance dependence of carrier transfer via tunneling processes from graphene quantum dots to InGaN quantum well**, Tzu-Neng Lin, Svette Reina Merden S. Santiago, Ji-Lin Shen, Chung Yuan Christian Univ. (Taiwan) [10672-146]
- Propagation of surface helicons in a semiconductor**, Valentin A. Tolkachev, Chelyabinsk State Univ. (Russian Federation); Igor V. Bychkov, Dmitry A. Kuzmin, Chelyabinsk State Univ. (Russian Federation) and South Ural State Univ. (Russian Federation); Vladimir G. Shavrov, Kotelnikov Institute of Radio Engineering and Electronics of Russian Academy of Sciences (Russian Federation); Olga Kharitonova, Chelyabinsk State Univ. (Russian Federation) [10672-147]
- Chirality and discrete diffraction in nonlinear Mathieu lattices**, Marius Rimmer, Alessandro Zannotti, Westfälische Wilhelms-Univ. Münster (Germany); Jadranka Vasiljevic, Dejan V. Timotijevic, Dragana M. Jović Savić, Univ. of Belgrade (Serbia); Cornelia Denz, Westfälische Wilhelms-Univ. Münster (Germany) [10672-148]
- Helium ion beam fabrication of nanofiber Bragg cavities**, Andreas W. Schell, ICFO - Institut de Ciències Fotòniques (Spain); Hideaki Takahima, Hirogona Maruya, Atsushi Fukuda, Kyoto Univ. (Japan) [10672-149]
- Tailored orbital and spin energy flow structures for advanced optical trapping**, Eileen Otte, Eric Asché, Ramon Runde, Cornelia Denz V, Westfälische Wilhelms-Univ. Münster (Germany) [10672-150]
- Compact Bloch surface waves devices based on multimode interference effect**, Kirill Safronov, Ksenia A. Abrashitova, Dmitry N. Gulkin, Natalia Kokareva, Ilya Antropov, Vladimir O. Bessonov, Andrey A. Fedyanin, M.V. Lomonosov Moscow State Univ. (Russian Federation) [10672-151]
- Temperature-dependent photoluminescence in nitrogen-doped graphene quantum dots**, Svette Reina Merden S. Santiago, Tzu-Neng Lin, Ji-Lin Shen, Chung Yuan Christian Univ. (Taiwan) [10672-152]
- A software for the simulation of light scattering by many particles in planarly layered media**, Amos Egel, Dominik Theobald, Guillaume Gomard, Uli Lemmer, Karlsruhe Institut für Technologie (Germany) [10672-153]
- GaP-on-insulator as a platform for nonlinear photonics**, Simon Hönl, Katharina Schneider, IBM Research - Zürich (Switzerland); Pol Welter, IBM Research - Zurich (Switzerland) and ETH Zurich (Switzerland); Yannick Baumgartner, Herwig Hahn, Lukas Czornomaz, IBM Research - Zürich (Switzerland); Dalziel J. Wilson, IBM Research - Zurich (Switzerland) and École Polytechnique Fédérale de Lausanne (Switzerland) [10672-154]
- Microwave surface plasmon-polariton resonances in VO₂ during metal-insulator phase transition**, Dmitry A. Kuzmin, Igor V. Bychkov, Chelyabinsk State Univ. (Russian Federation) and South Ural State Univ. (Russian Federation); Alexander P. Kamantsev, Victor V. Koledov, Dmitry S. Kuchin, Alexey V. Mashirov, Vladimir G. Shavrov, Kotelnikov Institute of Radio Engineering and Electronics of Russian Academy of Sciences (Russian Federation) [10672-155]

Chirality and discrete diffraction in nonlinear Mathieu lattices

M. Rimmmer¹, A. Zannotti¹, J. M. Vasiljevic², D. V. Timotijevic^{2,3}, D. M. Jovic Savic², and C. Denz¹

¹Institute of Applied Physics and Center for Nonlinear Science (CeNoS), University of Münster, 48149 Münster, Germany

²Institute of Physics, University of Belgrade, P.O. Box 68, 11001 Belgrade, Serbia

³Science Program, Texas A&M University at Qatar, P.O. Box 23874 Doha, Qatar

Non-diffracting beams are highly relevant in optics and atom physics, particularly because their transverse intensity distributions propagate unchanged for hundreds of diffraction lengths. Thus, they feature applications in free-space wireless communications, optical interconnections, long-distance laser machining, and surgery. Four different fundamental families of propagation invariant light fields exist. They distinguish in the underlying real space coordinate system: Discrete, Bessel, Weber, and Mathieu non-diffracting beams. Latter ones obey the Helmholtz equation in elliptic cylindrical coordinates and are therefore best suited to address physical effects in elliptical coordinates.

Mathieu beams are classified according to their symmetry properties as even and odd. Their transverse discrete intensity distributions in elliptical or hyperbolical geometries can be shaped by their order and an ellipticity parameter. These real-valued beams have only discrete spatial phase distributions. In contrast, so called elliptical and helical Mathieu beams are obtained as complex superpositions of appropriate even and odd Mathieu beams, thus showing outstanding continuously modulated spatial phase distributions that act as orbital angular momenta, associated with a transverse energy flow.

In our contribution we investigate and control the nonlinear optical induction of photonic Mathieu lattices in photosensitive media. As flexible material we chose a photorefractive SBN crystal, showing a non-local, anisotropic nonlinearity.

Focusing on elliptic Mathieu beams, during linear propagation their transverse energy redistribution along elliptic paths is compensated in each point, enabling for an invariant transverse intensity distribution. However, this energy flow withstands a direct observation. We demonstrate that their nonlinear self-action in SBN breaks this sensitive equilibrium. Consequently, a new type of rotating beam formation arises with high intensity filaments corresponding to the energy flow in an enforced preferential direction. This process is beneficially applied to realize chiral twisted photonic refractive index structures with a tunable ellipticity.

Further, we present our studies on the nonlinear dynamics of discrete Mathieu beams in SBN, showing examples of appropriate fundamental even Mathieu beams in order to realize one- and two-dimensional transverse lattices. The nonlinear optical induction process leads to the formation of discrete refractive index lattices and a self-interaction of the writing Mathieu beams with the realized photonic structure, capable of altering the writing beams' propagation similar to the well-known linear discrete diffraction. Controlling the strength of the nonlinearity allows tailoring the degree of diffraction. Moreover, probing the lattice linearly with Gaussian beams and tunable incident angles reveals the signature of discrete and anomalous diffraction. This allows to control the strength of diffraction, such that under certain tilts, the probing beams may cross the lattice diffractionless.

Our investigations both represent individual contributions towards the realization of advanced complex waveguiding in photorefractive crystals.

Realizing aperiodic photonic lattices by synthesized Mathieu-Gauss beams

J. M. Vasiljević¹, Alessandro Zannotti², D. V. Timotijević^{1,3}, Cornelia Denz², D. M. Jović Savić¹

¹Institute of Physics, University of Belgrade, P.O. Box 68, 11001 Belgrade, Serbia

²Institute of Applied Physics and Center for Nonlinear Science (CeNoS), Westfälische Wilhelms-Universität Münster, 48149 Münster, Germany

³Science Program, Texas A&M University at Qatar, P.O. Box 23874 Doha, Qatar

e-mail: jadranka@ipb.ac.rs

Over the years, non-diffracting wave configurations have drawn considerable attention, particularly in the areas of optics, atom physics, biophysics, as well as optical tweezing [1], and nonlinear optics [2, 3]. The interest in such optical waves is due to the fact that, their transverse intensity distributions propagate unchanged for hundreds of diffraction lengths. The potential of non-diffracting structures is of significant importance for advances in discrete and nonlinear modern photonics [4, 5]. One prominent class of non-diffracting waves is given by Mathieu beams, which appear as translationally invariant solution of the Helmholtz equation in elliptic cylindrical coordinates.

Synthesizing two or more non-diffracting Mathieu-Gauss (MG) beams, we demonstrate a powerful new approach for the creation of two-dimensional (2D) aperiodic photonic lattices, in a single writing process in parallel. Depending on the beam configurations of coherently superimposed MG beams, their mutual distances, angles of rotation or phase relations we are able to realize transverse invariant propagating intensity distributions capable to optically induce corresponding refractive index lattices in photosensitive media. Our approach features the fabrication of versatile aperiodic lattices with controllable properties as well as quasi one-dimensional structures. Our results and methods enable further investigations of light propagating in such aperiodic photonic lattices, and could find applications in modern optical information processing.

REFERENCES

- [1] V. Garcés-Chávez, D. McGloin, H. Melville, W. Sibbett, and K. Dholakia, Nature 419, 145 (2002).
- [2] J.W. Fleischer, M. Segev, N. K. Efremidis, and D. N. Christodoulides, Nature 422, 147 (2003).
- [3] H. Martin, E. D. Eugenieva, and Z. Chen, Phys. Rev. Lett. 92, 123902 (2004).
- [4] F. Diebel, B. M. Bokić, M. Boguslawski, A. Piper, D. V. Timotijević, D. M. Jović, and C. Denz, Phys. Rev. A 90, 033802 (2014).
- [5] F. Diebel, B. M. Bokić, D. V. Timotijević, D. M. Jović Savić, and C. Denz, Opt. Express 23, 24351 (2015).

We have also found a PBG fiber and a gas configuration whose characteristics permit the propagation of such stable solitons. Nevertheless, the linear gain, that is possible because the gas is only confined in the hollow core but not in the cladding holes, brings background instability.

Here, we systematically address the configurations of gases confined in PBG fibers that are more suitable for stable dissipative solitons, studying the dependence of sign and magnitude of the equation parameters with the experimental conditions. Moreover, we will obtain a propagation equation in fourth order which introduces a delayed Raman scattering term. This new term creates a new branch of solutions that exist and are stable in a limited range of the parameter space for which there is linear loss, so that, the background is stable.

REFERENCES

- [1] T. Hong, Phys. Rev. Lett. 90, 183901 (2003).
- [2] C. Hang, V. V. Konotop, Phys. Rev. A 81, 053849 (2010).
- [3] Y. Wu, L. Deng, Phys. Rev. Lett. 93, 143904 (2004).
- [4] J. Xu, G. Huang, Opt. Exp. 2, 5149 (2013).
- [5] Y. Zhang et al., Phys. Rev. A 82, 053837 (2010).
- [6] Z. Wu et al., Opt. Exp. 23, 8430 (2015).
- [7] M. Facão et al., Phys. Rev. A 91, 013828 (2015).

Light propagation in deterministic aperiodic Fibonacci waveguide arrays

J. M. Vasiljević, N. M. Lučić, D. V. Timotijević, A. Piper, D. Ž. Grujić,

D. V. Pantelić, B. M. Jelenković and D. M. Jović Savić

Institute of Physics, University of Belgrade, P.O. Box 68, 11001 Belgrade, Serbia

e-mail: jadranka@ipb.ac.rs

During the 1980s quasi-crystallographic structures in solid state physics fundamentally amazed the scientific community [1], and inspired a new field of research in optics and photonics. Owing to the analogy of photonic lattices to solid state systems, the first optical experiments were implemented analyzing aperiodic media [2]. Irregular photonic lattices are of great interest as these structures offer proper band gaps where propagation is forbidden while translation invariance and thus the general scheme of Bloch wave propagation within periodic arrangements are broken. Asking for aperiodic structures rapidly the nomenclature of Fibonacci grating came up for this often is referred to as the embodiment of irregularity [3,4]. Generally spoken, the research field of aperiodic lattices is a fertile topic [5] as these structures offer the possibility of light localization in deterministic disordered structures that are settled between periodic and disordered systems [6]. Light localization in quasi-periodic photonic lattices is observed in Aubry André model and also realized experimentally in AlGaAs substrate [7].

We extend these concepts to quasi-periodic Fibonacci waveguide arrays, considering light propagation along waveguides. We fabricate the array of identical waveguides (identical refractive index profile) in Fe:LiNbO₃ crystal. The distance between successive waveguides is modulated in Fibonacci manner. This means that the sequence of separations consists of two elements, A and B, lined in such a way to make Fibonacci word. We have analyzed experimentally and numerically how various incident beam positions influence propagation and localization characteristics and compare it with appropriate periodic waveguide arrays. In general, we find the beam expansion is slowed down in quasi-periodic Fibonacci waveguide arrays, and localization properties in such lattice are closer to a random than periodic lattice. However, with a modification of the refractive index variation, the localization effects are observed for shorter propagation distances by increasing refractive index variation.

REFERENCES

- [1] D. Shechtman et al., Phys. Rev. Lett. 53, 1951 (1984).
- [2] D. Levine, P. J. Steinhardt, Phys. Rev. Lett. 53, 2477 (1984).
- [3] G. Gumbs, M. K. Ali, Phys. Rev. Lett. 60, 1081 (1988).
- [4] E. L. Albuquerque, M. G. Cottam, Phys. Rep. 376, 225 (2003).
- [5] Z. V. Vardeny, A. Nahata, A. Agrawal, Nat. Photon. 7, 177 (2013).
- [6] A. Lagendijk, B. van Tiggelen, D. S. Wiersma, Phys. Today 62, 24 (2009).
- [7] Y. Lahini et al., Phys. Rev. Lett 103, 013901 (2009).

Counterpropagating optical solitons in PT symmetric photonic lattices

M. S. Petrović ^{1,2}, A. I. Strinić ^{2,3} and M. R. Belić ²

¹ Institute of Physics, PO Box 57, 11001 Belgrade, Serbia

² Texas A&M University at Qatar, PO Box 23874, Doha, Qatar

³ Institute of Physics, University of Belgrade, PO Box 68, 11080 Belgrade, Serbia

e-mail: petrovic@ipb.ac.rs

We construct solitonic solutions for the system of two optical beams propagating in opposite directions [1, 2] in parity-time (PT) symmetric [3, 4] photonic lattices by using modified Petviashvili method [5]. Our system support PT symmetric fundamental solitons, as well as solitary vortices. We propagate them and investigate their basic characteristics. We report power transfer between counterpropagating beams and symmetry breaking (or split-up) transition.

REFERENCES

- [1] M. Petrovic et al., Phys. Rev. Lett. 95, 053901 (2005).
- [2] M. S. Petrovic et al., Laser Photonics Rev. 5, 214 (2011).
- [3] C. M. Bender, S. Boettcher, Phys. Rev. Lett. 80, 5243 (1998).
- [4] C. M. Bender, Rep. Prog. Phys. 70, 947 (2007).
- [5] V. I. Petviashvili, Fiz. Plazmy 2, 469 (1976) [Sov. J. Plasma Phys. 2, 257 (1976)].



Република Србија
Универзитет у Београду
Физички факултет
Д.Бр.2014/8005
Датум: 15.01.2019. године

На основу члана 161 Закона о општем управном поступку и службене евиденције издаје се

УВЕРЕЊЕ

Васиљевић (Милољуб) Јадранка, бр. индекса 2014/8005, рођена 27.05.1990. године, Краљево, Краљево-град, Република Србија, уписана школске 2018/2019. године, у статусу: самофинансирање; тип студија: докторске академске студије; студијски програм: Физика.

Према Статуту факултета студије трају (број година): три.
Рок за завршетак студија: у двоструком трајању студија.

Ово се уверење може употребити за регулисање војне обавезе, издавање визе, права на децији додатак, породичне пензије, инвалидског додатка, добијања здравствене књижице, легитимације за повлашћену вожњу и стипендије.

Овлашћено лице факултета



Мосеков



РЕПУБЛИКА СРБИЈА

УНИВЕРЗИТЕТ У КРАГУЈЕВЦУ

ПРИРОДНО-МАТЕМАТИЧКИ ФАКУЛТЕТ У КРАГУЈЕВЦУ

Оснивач: РЕПУБЛИКА СРБИЈА

Дозволу за рад број: 612-00-00762/2010-04 од 30. 12. 2010. године издало је

Министарство просвете Републике Србије, Београд



ДИПЛОМА

ЈАДРАНКА, Милољуб, ВАСИЉЕВИЋ

рођена 27. 05. 1990. године у Краљеву,

општина Краљево, Република Србија,

уписана школске 2009/2010. године, а дана 03. 10. 2013. године завршила је

основне академске студије ПРВОГ СТЕПЕНА на студијском програму

ФИЗИКА

обима 240 (двеста четрдесет) бодова ЕСПБ

са просечном оценом 9,51 (девет и 51/100).

На основу тога издаје се ова диплома о стеченом ВИСОКОМ ОБРАЗОВАЊУ

и стручном називу **ДИПЛОМИРАНИ ФИЗИЧАР**

ОА-253-49/14-09, 15. 04. 2014. године

У Крагујевцу

Декан
Драгослав Никезић
Проф. др Драгослав Никезић

Ректор
Слободан Арсенијевић
Проф. др Слободан Арсенијевић

ОА – 002777



РЕПУБЛИКА СРБИЈА

УНИВЕРЗИТЕТ У КРАГУЈЕВЦУ

ПРИРОДНО-МАТЕМАТИЧКИ ФАКУЛТЕТ У КРАГУЈЕВЦУ

Оснивач: РЕПУБЛИКА СРБИЈА

Дозволу за рад број: 612-00-00762/2010-04 од 30. 12. 2010. године издало је
Министарство просвете Републике Србије, Београд



ДИПЛОМА

ЈАДРАНКА, Милољуб, ВАСИЉЕВИЋ

рођена 27. 05. 1990. године у Краљеву,

општина Краљево, Република Србија,

уписана школске 2013/2014. године, а дана 01. 10. 2014. године завршила је

мастер академске студије ДРУГОГ СТЕПЕНА на студијском програму

ФИЗИКА

обима 60 (шездесет) бодова ЕСПБ

са просечном оценом 9,50 (девет и 50/100).

На основу тога издаје се ова диплома о стеченом ВИСОКОМ ОБРАЗОВАЊУ

и академском називу **МАСТЕР ФИЗИЧАР**

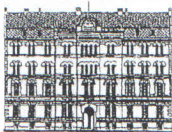
МА-160-106/15-09, 15. 04. 2015. године

У Крагујевцу

Декан
S. Ј. Јаковић
Проф. др Срећко Трифуновић

Ректор
С. Ј. Јаковић
Проф. др Слободан Арсенијевић

МА – 001726



ДОКТОРСКЕ СТУДИЈЕ

ПРЕДЛОГ ТЕМЕ ДОКТОРСКЕ ДИСЕРТАЦИЈЕ КОЛЕГИЈУМУ ДОКТОРСКИХ СТУДИЈА

Школска година
20 18/20 19

Подаци о студенту

Име **Јадранка**
Презиме **Ваљевић**
Број индекса **8005 / 2014**

Научна област дисертације

Нелинеарна фотоника
Квантна оптика и ласери

Подаци о ментору докторске дисертације

Име **Драгана**
Презиме **Јовић Савић**

Научна област **нелинеарна фотоника**

Звање **научни саветник**

Институција **Институт за физику у Земуну**

Предлог теме докторске дисертације

Наслов

**Промитрање, локализација и контрола светлосни у
Макрјевим решеткама**

Уз пријаву теме докторске дисертације Колегијуму докторских студија, потребно је приложити следећа документа:

1. Семинарски рад (дужине до 10 страница)
2. Кратку стручну биографију писану у трећем лицу једнине
3. Фотокопију индекса са докторских студија

Датум	22.04.2019.	Потпис ментора	Драгиша Јован Ћеб
Потпис студента	ТВасиљевић		

Мишљење Колегијума докторских студија

Након образложења теме докторске дисертације Колегијум докторских студија је тему

прихватио

није прихватио

Датум

Продекан за науку Физичког факултета

8. 5. 2019

Симон Ђорђевић